Quaternary Science Reviews xxx (2012) 1–22

Contents lists available at SciVerse ScienceDirect

Quaternary Science Reviews

journal homepage: www.elsevier.com/locate/quascirev

The Holocene sedimentary history of the Kangerlussuaq Fjord-valley fill, West Greenland

Joep E.A. Storms [a,*], Ilja L. de Winter [a], Irina Overeem [b], Guy G. Drijkoningen [c], Holger Lykke-Andersen [d]

[a] Department of Geotechnology, Section Applied Geology, Delft University of Technology, The Netherlands
[b] INSTAAR, University of Colorado, Boulder, USA
[c] Department of Geotechnology, Section Applied Geophysics, Delft University of Technology, The Netherlands
[d] Department of Earth Sciences, University of Aarhus, Denmark

ARTICLE INFO

Article history:
Received 8 April 2011
Received in revised form
15 December 2011
Accepted 16 December 2011
Available online xxx

Keywords:
Kangerlussuaq
Deglaciation
Søndre Strømfjord
Holocene
Watson River
Glacial fjord infill
Greenland Ice Sheet
Ground penetrating radar
Sedimentology

ABSTRACT

West Greenland has been intensively studied to reconstruct and better understand past relative sea level changes and deglacial history. This study extends these efforts by linking sea level and deglacial history to the sedimentary infill successions of Kangerlussuaq Fjord and associated landward valleys. Based on published and new land- and sea-based geophysical data, radiocarbon dates and geological observations we have characterized the infill and reconstructed the sedimentation history during the Holocene.

Based on a revised sea level curve and data presented in this paper we defined three depositional phases. Phase I (>7000 yr BP) is represented by dominant glaciomarine deposition associated with a tide-water glacier system. As the Greenland Ice Sheet (GIS) continued to retreat it became land based. During phase II (7000–1500 yr BP) two separate depocenters formed. Keglen delta depocenter arose from a temporary stabilization phase of the GIS and prograded rapidly over the glaciomarine deposits of Phase I. Further inland, proglacial lake formation and subsequent sedimentary infill associated with the ongoing GIS retreat is represents the second depocenter. The Watson River connected both depocenters by a flood plain which transferred sediment from the GIS to the Keglen delta. Ongoing sea level fall due to glacio-isostastic uplift combined with a gradually cooler and dryer climate resulted in terrace formation along the Watson River flood plain. Around 4000 yr BP, the GIS margin reached its most landward location and began to advance to its present location. The final phase (Phase III; <1500 yr BP) is represented by a stabilized GIS position and a relative sea level rise which led to aggrading conditions near the present-day delta plain of Watson River. Simultaneously, subaqueous channels were formed at the delta front by hyperpycnal flows associated with jökulhlaup events.

1. Introduction

Fjords and glacial valleys, carved into bedrock by repeated glaciations, are typically elongated basins which become major sediment sinks during deglaciations. Based on numerous seismic studies of Holocene fjord infills in Greenland (e.g. Ó Cofaigh et al., 2001; Desloges et al., 2002), Canada and Alaska (e.g. Gilbert, 1985; Carlson, 1989; Powell and Molnia, 1989; Eyles et al., 1991; Cai et al., 1997; Syvitski and Lee, 1997) and Norway (e.g. Aarseth, 1997; Lyså and Vorren, 1997; Plassen and Vorren, 2003; Lyså et al., 2004; Hansen et al., 2009), it is shown that pre-Holocene fjord and valley sediments are generally removed by glaciers during the preceding glacial period. This reset of fjord and valley sediment infill during each subsequent glacial cycle is characteristic for glaciogenic sedimentary basins.

While local non-glaciogenic sedimentary basin infill character is a function of local sea level and sediment supply, glaciogenic sedimentary basin infill is additionally affected by temporal ice margin shifts. This mechanism leads to rapid depocenter shifts (Corner, 2006). Furthermore, rapid local sea level change as well as fast uplift due to glacio-isostatic rebound contribute to this depocenter shift mechanism (e.g. Overeem and Syvitski, 2010). The sequence stratigraphic signature of glaciogenic basins is therefore different from non-glaciogenic basins (e.g. Corner, 2006). The stratigraphic signature of the infill is a function of the phase of deglacial processes (deglacial vs. postglacial) and associated depositional environment (e.g. ice-contact, glaciomarine, glaciolacustrine, fluvial, eolian, etc.).

Few studies have attempted to link the deglacial history to the infill history. Most fjord infill studies have focused on the

* Corresponding author. Tel.: +31 15 2784810; fax: +31 15 2783328.
E-mail address: j.e.a.storms@tudelft.nl (J.E.A. Storms).

0277-3791/$ – see front matter © 2012 Elsevier Ltd. All rights reserved.
doi:10.1016/j.quascirev.2011.12.014

stratigraphic architecture of the marine depositional environment using various seismic techniques and coring. Recently, land-based studies have focused on the terrestrial part of the valley infill (e.g. Helle, 2004; Eilertsen et al., 2006; Hansen et al., 2009; Overeem et al., in preparation) but only on rare occasions do studies integrate terrestrial and marine data (e.g. Eilertsen et al., 2005). The present study combines both on- and offshore data to ensure a complete interpretation of the infill history of Kangerlussuaq Fjord, West Greenland (Fig. 1) linked to its deglacial history.

Kangerlussuaq Fjord area has been extensively studied since the 1970's (e.g. Sugden, 1972; Ten Brink, 1974, 1975; Ten Brink and Weidick, 1974; Kelly, 1985; Weidick, 1985, 1993; Eisner et al., 1995; Van Tatenhove, 1995; Van Tatenhove et al., 1996) which has led to a good understanding of regional deglaciation history based on radiocarbon dated material from moraine systems and associated glaciomarine deposits (Van Tatenhove et al., 1996), eolian (Willemse and Törnqvist, 1999) and lake deposits (Aebly and Fritz, 2009). This makes Kangerlussuaq an ideal study area to untangle the relation between the deglacion and the sedimentation history. Furthermore, Western Greenlandic fjords have experienced a major readvance of the Greenland Ice Sheet (GIS) between approximately 4000 yr BP and 3000–1000 yr BP (Kelly, 1988; Scholz and Grottenthaler, 1989; Weidick, 1993; Van Tatenhove et al., 1996). This readvance is expected to have had a large impact on the sediment infill history.

The goals of this research are (1) to understand the Kangerlussuaq Fjord and valley infill as a function of glacier fluctuations, sea level change and shifts in depocenter through time, (2) to reconstruct local deposition rates, (3) to characterize the fjord infill and to link on- and offshore data, and (4) to understand the effect of neoglacial ice readvance on the depositional system. To achieve these goals a suite of research techniques was used, including geophysical surveying and radiocarbon dating.

2. Setting

2.1. Valley systems and glaciers

Kangerlussuaq Fjord, also known as Søndre Strømfjord, is WSW-ENE oriented and approximately 175 km long. The fjord is carved in Precambrian rock, mostly gneiss, and varies in width from 4.5 km near the village of Kangerlussuaq (Fig. 2) to about 2 km near the connection to Davis Strait (Bonow et al., 2006). The depth of the present-day fjord varies from tenths of meters in the outer fjord to over 300 m eastward of the Sarfartôq sill. Sukkertoppen ice cap (Fig. 1) supports a number of small outlet glaciers which discharge sediment in Kangerlussuaq Fjord. A valley system is present between the fjord terminus and the present position of the Greenland Ice Sheet (Fig. 2).

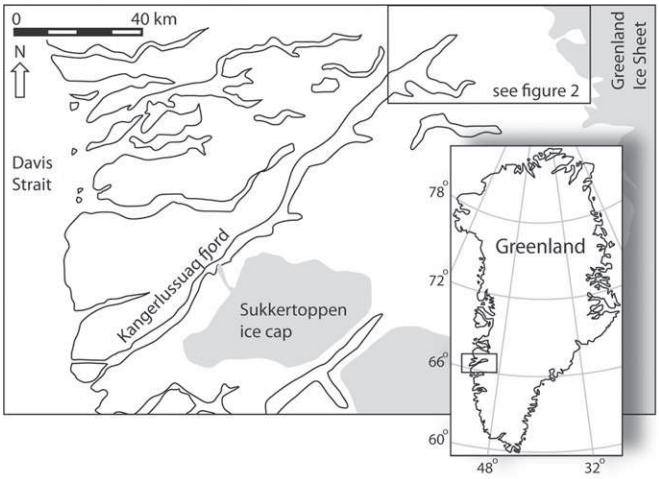

Fig. 1. Overview of the Kangerlussuaq Fjord area, west Greenland.

2.2. Marine limit

For the Kangerlussuaq area, Ten Brink (1974) determined the marine limit at 40 ± 5 m based on the elevation of the top of the marine clay terraces near Watson Bridge (Fig. 2). The use of marine clays as a marker for the marine limit is ambiguous since they do not refer to a palaeo coastline position. As such, marine clays only refer to a minimum marine limit.

2.3. Climate

Observations from the Danish Meteorological Institute show the mean annual temperature between 1980 and 1999 at Kangerlussuaq Airport (which lies 50 km north of the Arctic Circle and at the lee side of the Sukkertoppen mountain range) was −0.6 °C, with positive mean monthly temperatures between May and September. Mean annual precipitation is a mere 149 mm per year, of which 65% falls between May and October during on average 23 days. Toward the west precipitation rates are much higher.

Sea ice occupies the fjord between October and May. Based on harmonic tidal calculations (taken from http://www.tide-forecast.com/locations/CampLloyd-SondreStromfjord-Greenland/tides/latest) it is estimated that the tidal range is about 3.2 m near Camp Lloyd (Kangerlussuaq Harbor) and 3.4 m near Davis Strait (Fishermans Harbor).

2.4. Glaciofluvial regime

Four main tributary valleys connect to the Kangerlussuaq Fjord. This study will focus on the most northeastern tributary systems which are drained by the Watson River. Northeastward of the present-day Watson delta (near the village of Kangerlussuaq) the fjord extends about 25 km landwards into a valley basin. This valley basin is located landward of the current marine limit (Fig. 2). In this study we focus on the northern branch of the valley basins (Sandflugtdalen). At present, two glacial tongues of the GIS drain to Sandflugtdalen; Russell Glacier in the north and Leverett Glacier in the south. The Watson River runs ~31 km from the ice margin before converging with the Ørkendalen River, prior to entering Kangerlussuaq Fjord. The Ørkendalen River flows 41 km from the ice sheet margin to the convergence. The flood plain is only active during the melt season (May–September), while the flood plain substrate is frozen during the fall, winter and early spring months. In melt season the flood plain drains glacial melt water. The water discharge ranges between 50 and 500 $m^3\ s^{-1}$ (Mernild and Hasholt, 2009). The associated suspended sediment concentration ranges between 1000 and 2500 mg L^{-1}. The amount of summer rain fall that contributes to river discharge is insignificant. McGrath et al. (2010) showed that the present-day Watson River has a limited response to daily precipitation events. Summer precipitation in the Watson River catchment only accounts for less than 30 $m^3\ s^{-1}$ water discharge. Therefore the present-day hydrograph is driven by melt of the GIS margin, and is predominantly a function of air temperature.

In addition to the daily variation in discharge due to meteorological fluctuations (Mernild and Hasholt, 2009), the discharge is also characterized by the occurrence of large, short-term fluctuations of which the origin is twofold. Russell (1989, 2007 and 2009) describes Jökulhlaup events of catastrophic scale (with an

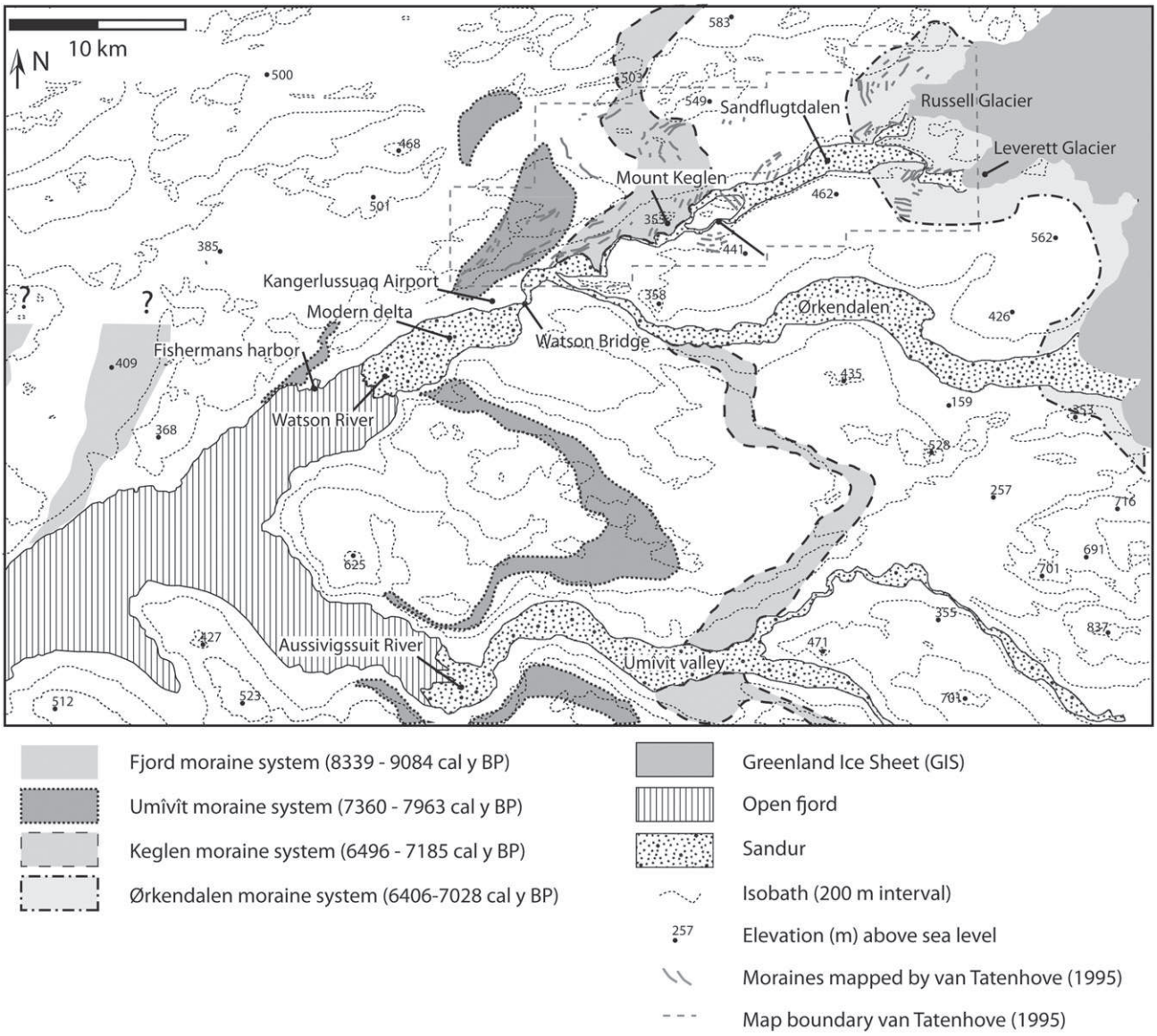

Fig. 2. Detailed composite map showing regional moraine systems, local moraines, the position of the sandur and delta plains and the location of the present Greenland Inland Sheet margin in the research area. Map based on data from Van Tatenhove et al. (1996), Ten Brink, 1975. Sarfartôq-Advedtleq moraine system (8896–9727 cal yr BP) is not shown on the map. It is located along the hills bordering Kangerlussuaq Fjord ±70 southwestward of Watson Bridge.

estimated maximum discharge of 1800 $m^3 s^{-1}$), occurring every so many years, which lead to morphological changes, erosion and deposition within a time period of days. The Jökulhlaups are caused by sudden drainage of large ice-dammed lakes fringing the GIS. Similar events, with much smaller magnitude but higher return frequency, are induced by ice-cliff collapse of the Russell glacier (Russell et al., 1995). Large chunks of collapsed glacier ice temporary dam the Watson River, which undermines the ice front, after which the ponded water breaks out and flood the delta plain. The resultant fluctuations are less than 2 h in duration, with a maximum fluctuation magnitude of 50 $m^3 s^{-1}$.

2.5. Regional deglaciation history

The Kangerlussuaq Fjord area was fully glaciated at the onset of the Holocene (Funder and Hansen, 1996). The early Holocene is characterized by a regional warm period showing mean annual temperatures in the first millennia of the Holocene at least 1 °C warmer than today over central Greenland (e.g. Alley et al., 1997; Dahl-Jensen et al., 1998; Vinther et al., 2009), and 5 °C warmer summers than today on Baffin Island (Axford et al., 2009). An overall higher temperature with large fluctuations combined with lower than present precipitation-evaporation ratio due to a decreased mean annual precipitation (McGowan et al., 2003; Anderson and Leng, 2004; Aebly and Fritz, 2009) led to fluctuating retreating glaciers that formed a series of regional moraine systems. In addition, numerous local terminal and lateral moraines have been mapped and dated located between Mount Keglen and the present-day position of the GIS which cannot be linked to regional moraine systems (Fig. 2) (Van Tatenhove et al., 1996).

Ten Brink and Weidick (1974) mapped and dated the regional moraine systems (Fig. 2). The age ranges we report here are calibrated versions of the original radiocarbon dates as reported by Ten Brink and Weidick (1974) including one standard deviation error: Sarfartôq-Advedtleq (8896–9727 cal yr BP), Fjord (8339–9084 cal yr BP), Umîvît (7360–7963 cal y BP), Keglen

Please cite this article in press as: Storms, J.E.A., et al., The Holocene sedimentary history of the Kangerlussuaq Fjord-valley fill, West Greenland, Quaternary Science Reviews (2012), doi:10.1016/j.quascirev.2011.12.014

(6496–7185 cal y BP) and Ørkendalen (6406–7028 cal y BP). Although Ten Brink (1975) and Ten Brink and Weidick (1974) describe the Umîvît and Keglen moraine systems as individual systems, Van Tatenhove et al. (1996) merged them into one large moraine system due to their short distance and overlapping ages.

A local ice cap persists south of Kangerlussuaq Fjord (Sukkertoppen, Fig. 1). This ice cap is believed to follow the regional deglaciation trend of the GIS (Sugden, 1972), but indications exist that it may have affected the regional deglaciation through blockage of Kangerlussuaq Fjord by glaciers emerging from Sukkertoppen ice cap (Van der Meer et al., 1993, 1994).

2.6. Neoglacial developments

After the formation of the Ørkendalen moraine system the ice margin continued to retreat. During this retreat frequent, but temporary, standstills occurred, as testified by moraines systems preserved along the northern fringe of Sandflugtdalen (Van Tatenhove et al., 1996). Weidick (1993) suggested that the maximum retreat was about 15 km landward from the present ice margin around 4.0 ± 0.9 cal ky BP. Numerical ice sheet models (e.g. Tarasov and Peltier, 2003; Fleming and Lambeck, 2004; Simpson et al., 2009) confirm the retreat hypothesis but show a wide variability in timing and extent of the GIS retreat and subsequent Neoglacial advance (Long et al., 2009; Briner et al., 2010). According to Weidick (1993) the ice margin reached its present-day position about 3.0 cal ky BP where it remained fairly stable since. Later work from Foreman et al. (2007) suggests that the ice margin following the Neoglacial event reached its maximum extent approximately 2.0 cal ky BP. They also argue that this maximum expansion of the Neoglacial ice margin coincides with the Little Ice Age (LIA) maximum extent (0.7–0.1 cal ky BP).

2.7. Glacio-isostatic adjustments

2.7.1. Emergence curve

Based on radiocarbon dated marine shells retrieved from strandlines, Ten Brink (1974) constructed an emergence curve for the Umîvît and Kangerlussuaq Air base region (Fig. 2) for the early and mid Holocene (>5000 y BP). Recently, Bierman et al. (2010) published new independent data points which confirmed this emergence curve using 10-Be datings at the bedrock sill under Watson Bridge. Ten Brink (1974, 1975) did not consider the effects of the Neoglacial advance of the ice margin and as a result assumed that the exponential emergence curve approached 0 m uplift rate for present-day deposits.

2.7.2. Neoglacial subsidence

Long et al. (2006) shows for Disko Bugt, an area approximately 200 km north of Kangerlussuaq, that sea level reached a minimum of −5 m around 2000 years ago. Other records of dated submerged landforms in western Greenland indicate a shift from a falling to a rising relative sea level 3000 years ago (Long et al., 2009). This shift in relative sea level is interpreted to record the combined glacio-tectonic effect of the expansion of the western GIS during Neoglaciation as well as the collapse of the peripheral forebulge that surrounded the former Laurentide Ice Sheet (Tarasov and Peltier, 2002; Fleming and Lambeck, 2004; Long et al., 2010).

Recent measurements near Kangerlussuaq using repeated geodetic/DGPS observations (Dietrich et al., 2005) show that

Table 1
Radiocarbon datings analyzed for this study.

Laboratory number	Location	Core/Location name	Sample position relative to MSL (m)	Material	Conventional age (14C yr B.P.)	Age (cal yr B.P.), One standard deviation
Beta-259662	66°50′07.8″N 51°21′07.8″W	92GDW05	−252.43	Roots	40 ± 40	251–modern
Beta-259663	66°26′03.2″N 52°22′34.6″W	92GDW17	−51.64	Shell	480 ± 40	n/a
Beta-259664	66°26′03.2″N 52°22′34.6″W	92GDW17	−54.37	Shell	780 ± 40	422–147
Beta-259665	66°10′14.6″N 53°02′31.5″W	92GDW19	−39.7	Shell	490 ± 40	n/a
Beta-259666	66°10′14.6″N 53°02′31.5″W	92GDW19	−41.16	Shell	1630 ± 40	938–1165
Beta-259668	66°35′09.2″N 52°00′45.2″W	92PCM08	−282.76	Roots	170 ± 40	Modern–285
Beta-259669	66°35′09.2″N 52°00′45.2″W	92PCM08	−289.06	Shell	720 ± 40	74–322
Beta-259670	66°31′08.3″N 52°05′20.2″W	92PCM09	−151.23	Shell	760 ± 40	142–394
Beta-259671	66°31′08.3″N 52°05′20.2″W	92PCM09	−158.50	Shell	1090 ± 40	485–642
Beta-259673	66°43′31.1″N 51°32′56.0″W	92PCM30	−289.03	Roots/wood	750 ± 40	667–722
Curl-10994	67°0′12.585″N 50°45′56.979″W	C14_1_GR_10	+12.0	Shell	6275 ± 15	6455–6692
Curl-10997	67°0′12.681″N 50°45′56.731″W	C14_2_GR11	+12.5	Shell	Modern	Modern
Curl-10990	67°0′12.681″N 50°45′56.731″W	C14_3_GR11	+12.0	Shell	7725 ± 20	7953–8159
Curl-10995	67°0′29.069″N 50°45′45.175″W	C14_4_GR31	+25.0	Shell	6430 ± 20	6639–6885
Curl-10988	66°59′57.197″N 50°40′50.904″W	C14_5a_GR87	+26.0	Shell	6245 ± 15	6425–6657
Curl-10986	66°59′57.197″N 50°40′50.904″W	C14_6_GR87	+13.0	Shell	6460 ± 15	6669–6916
Curl-11000	66°58′41.610″N 50°55′6.994″W	C14koepel	+46	Shell	7625 ± 15	7840–8059

Calibration using $R = 130 \pm 100$ Calib6.0 Marine09 data set for shells, Intcal09 database for roots/wood.

Please cite this article in press as: Storms, J.E.A., et al., The Holocene sedimentary history of the Kangerlussuaq Fjord-valley fill, West Greenland, Quaternary Science Reviews (2012), doi:10.1016/j.quascirev.2011.12.014

Table 2
Overview of radar facies for the 50 MHz data set.

Radar Facies (RF)	Maximum thickness	Description of reflection pattern	Interpretation
 RF1	30 m	Small-scale variability. Steeply dipping to sub horizontal and parallel. Discontinuous to continuous. Local diffractions.	Various *ice-contact* deposits, including large clasts to fine-grained sediments. (*IC*)
 RF2	15 m	Discontinuous, parallel to undulating. Locally inclined.	*Proximal glaciolacustrine* deposit affected by waterflow. Inclination depends on underlying morphology. (*GL-Pr*)
 RF3	40 m	Continuous, parallel. Locally inclined.	*Distal glaciolacustrine* deposit dominated by suspension fallout. No apparent waterflow. (*GL-Dis*)
 RF4	20 m	Discontinuous to continuous oblique to curved.	*Glaciofluvial delta* foresets to bottomset. (*GF*)

between 1995 and 2002 a steady subsidence rate of 3.1 mm/y occurs at Watson Bridge. Ten kilometers further seaward, at Kellyville (near Kangerlussuaq harbor), an independent GPS station gave similar results (Dietrich et al., 2005). We therefore assume that the subsidence is associated with the isostatic adjustment following the Neoglacial advance of the ice margin.

3. Methods and data acquisition

Ground penetrating radar and onshore seismic data were collected during field campaigns in April 2008. We collected elevation and positioning data using a commercial-grade WAAS GPS.

3.1. Ground penetrating radar

A total of 37 km of ground penetrating radar (GPR) profiles were collected. The frozen subsurface with a discontinuous thin snow cover ensured favorable GPR survey conditions. We collected low-frequency GPR data (50 and 100 MHz using a PulseEkko 100 system) and were able to image the full valley basin fill down to the bedrock interface. GPR – Common midpoint measurements were conducted in order to establish the wave velocity in the (partially) frozen substrate. Due to the consistent presence of the permafrost, the velocity profile was uniform and an overall velocity of 0.135 m/ns was used for the time-depth conversion. Problems with the electronics obscured the signal within the first ~150 ns by oversaturating (clipping) the received signal. This translates into a noisy upper part of the GPR profiles of about 20 m. However, data below this depth was of very good quality. Signal processing was applied with ReflexW software v4.5 (Sandmeier, 2007). The workflow involved dewow, Frequency-Wavenumber (F–K) and bandpass filtering and Kirchoff migration. The processed profiles were subsequently imported in the Schlumberger Petrel 2008 software for spatial interpretation (Afanasyev, 2009). Four radar facies have

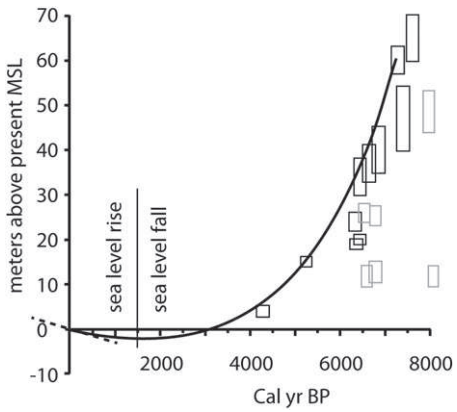

Fig. 3. Holocene sea level curve for the area near Watson Bridge based on calibrated radiocarbon dates from Ten Brink (1974; black boxes) combined with new calibrated radiocarbon dates (gray boxes) and recent subsidence measurements of 3.1 mm/y (see dotted line; Dietrich et al., 2005). The curve indicates a shift from sea level fall to rise conditions around 1500 cal y BP. See text for details.

Please cite this article in press as: Storms, J.E.A., et al., The Holocene sedimentary history of the Kangerlussuaq Fjord-valley fill, West Greenland, Quaternary Science Reviews (2012), doi:10.1016/j.quascirev.2011.12.014

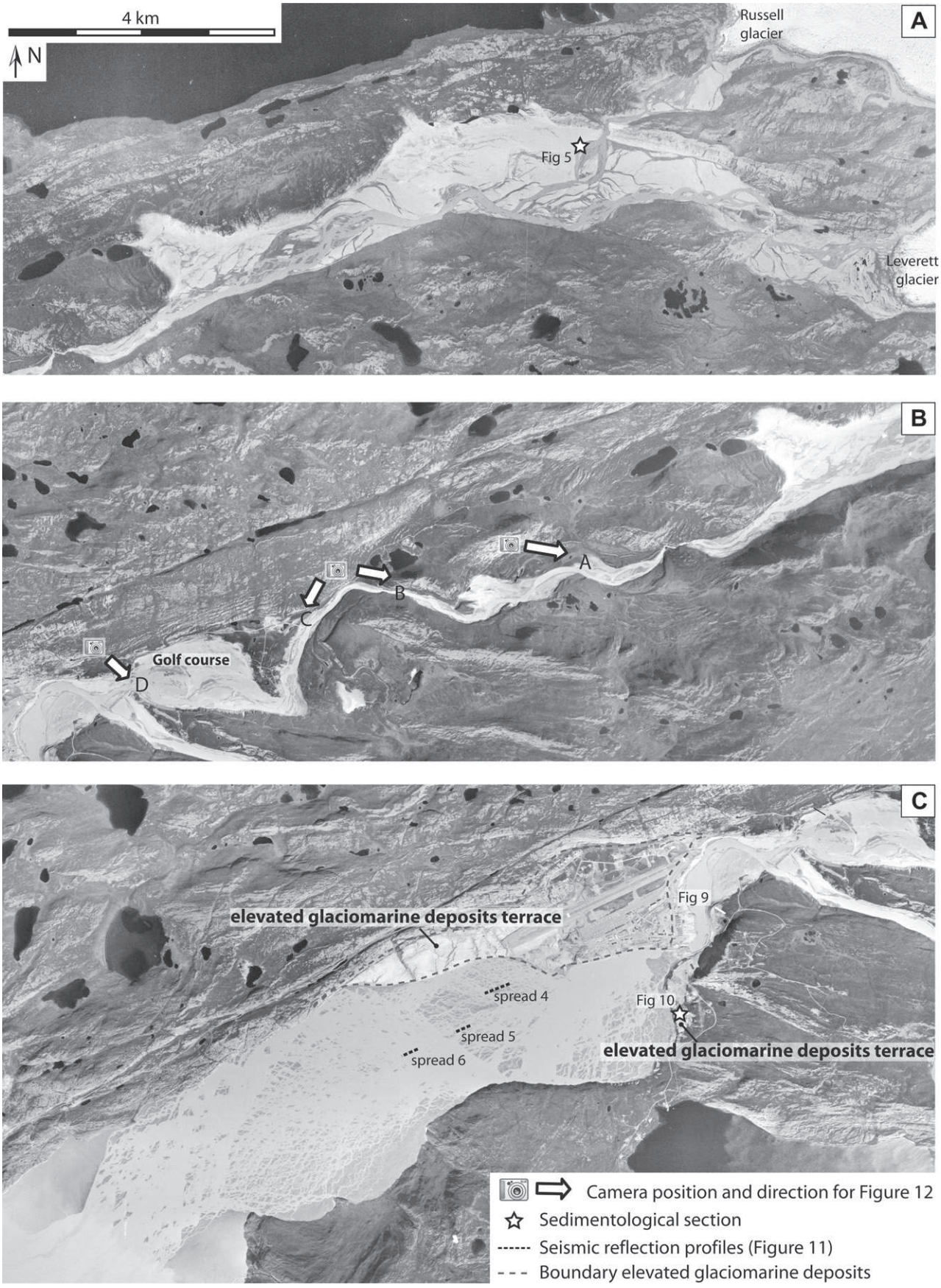

Please cite this article in press as: Storms, J.E.A., et al., The Holocene sedimentary history of the Kangerlussuaq Fjord-valley fill, West Greenland, Quaternary Science Reviews (2012), doi:10.1016/j.quascirev.2011.12.014

been identified for the 50 MHz data (Table 2) following the approach of Jol and Bristow (2003), Van Heteren et al. (1998) and Hansen et al. (2009) who define radar facies as 3D units composed of reflection patterns differing from those of adjacent units. While both processed and raw images were used for interpretation and radar facies classification, the radar profiles shown in this paper are post-processed using dewow and AGC gain only for consistency. No topographic correction has been applied because the vertical accuracy of the GPS (±5 m) was similar to the observed topographic variability along individual GPR lines.

3.2. Seismics

The seismic reflection survey consisted of 24 fixed 10 Hz vertical geophones (type SM4 manufactured by ION) with 2–4 m spacing and a moving source (5 kg hammer on metal plate). Seismic reflections were recorded with a 24-channel seismograph (type Geode manufactured by Geometrics). Spreads were collected from both valley infills at Sandflugtdalen and the modern delta. Although the approximated depth to bedrock in Sandflugtdalen as imaged by seismic and GPR data agreed, seismic data revealed much less stratigraphic detail than the GPR data. We therefore decided to focus the seismic profiling to the modern delta for the estimation of bedrock depths.

Offshore seismic data were collected in 2008 by Aarhus University, Denmark using a boomer system (Uniboom by EG&G) and operated at 100 J energy level, resulting in a 0.7–14.0 kHz frequency band. The data were recorded with the PC-based Chesapeake system.

3.3. Description of sedimentary sections

We described ~35 m of sedimentary logs along exposed terraces intersections and excavated 6 shallow (<1 m) soil pits. Typically we described mean grain size, sorting, roundness and bed thickness. If present we also characterized sedimentary structures and erosion surfaces.

3.4. Radiocarbon dating

We collected 17 samples for AMS radiocarbon dating (Table 1). Seven samples were collected from the raised marine terraces bordering the delta that consist of intact single-sided bivalves that were analyzed at the INSTAAR – Laboratory for AMS Radiocarbon Preparation and Research. In addition, ten samples for AMS radiocarbon dating (analyzed by Beta Analytic Inc.) were collected from pistoncore, vibracore and boxcore data that were retrieved in 1992 in Kangerlussuaq Fjord during the GIMEXMAR'92 cruise initiated by the Dutch Geological Survey (Oele, 1992). These cores were described in detail and sampled by Bakker (1996). Additionally, radiocarbon dates published in previous papers were-reassessed. All radiocarbon dates (new and from literature) were calibrated to calendar years using Calib 6.0html software with the MARINE09 calibration data set for shell samples and the INTCAL09 data set for wood or gyttja samples (Stuiver et al., 2005). Although the radiocarbon ages from Ten Brink (1975) and Ten Brink and Weidick (1974) have typical uncertainties of plus or minus 150 years for individual dated shell samples, we assume a larger uncertainty for the derived ages of moraine systems, which are often based on several dated shells. This way we include additional uncertainties of ±300 years in the interpretation between the inferred ages of shell samples and the formation or the moraine system. For marine samples (shells) we assumed a marine reservoir correction (Delta-R) value of 130 ± 100 based on Greenland data published by McNeely et al. (2006). We report the calibrated age range for one standard deviation uncertainty.

4. Revised sea level curve

For this study, a revised local sea level curve (Fig. 3) was constructed by combining the linear increase in subsidence rate from zero at the onset of the glacial advance 4000 y BP to 0.003 m/y at present with the calibrated radiocarbon dates of marine shells published by Ten Brink (1974) and new radiocarbon datings (this study, Table 1). The shells dated for this study show a significant offset from the original calibrated radiocarbon dates of Ten Brink (1974). This can be explained by presuming that these shells at the time of burial lived in a considerable water depth (>20 m). The new sea level curve shows that the regional relative sea level trend reversed around 1500 years ago from falling to rising. At that stage, sea level was about 2.5 m below present sea level.

5. Depositional development

In this section we will present data and interpretations leading to a reconstruction of the depositional development for the three main sediment depocenters: Sandflugtdalen, Keglen delta and the modern delta including Kangerlussuaq Fjord. Sandflugtdalen is located near the present-day GIS margin, Keglen delta is located between Mount Keglen and Watson Bridge while Kangerlussuaq Fjord represents the present-day delta and open fjord environment (Fig. 2).

5.1. Sandflugtdalen

5.1.1. Sedimentological data

A sedimentary succession exposed along a 12 m high terrace escarpment that separates a higher terrace from the modern flood plain, has been logged to characterize the uppermost part of the valley infill at Sandflugtdalen (see Fig. 4 for location, log in Fig. 5). The sedimentary log shows heterogeneous deposits with distinct decimeter to meter-scale layers of alternating well-sorted planar laminated or cross-bedded coarse sand, and very poorly sorted gravel with a sand matrix. The contacts are generally erosional. There are no obvious fining or coarsening upward trends. The pebbles and cobbles are well rounded and may exceed 15 cm in diameter. Grain sizes smaller than fine sand are not observed in the logged section.

5.1.2. Ground penetrating radar data and facies

The GPR data collected at Sandflugtdalen were classified into four radar facies (Table 2). Radar facies 1 (RF1) is characterized by small-scale variability in reflection patterns which includes steeply dipping to sub horizontal, discontinuous to continuous reflections with many local diffractions. Occasionally reflections may be parallel. Radar facies 2 (RF2) is characterized by discontinuous, parallel to undulating reflections. These reflections may be inclined. Radar facies 3 (RF3) is characterized by continuous, parallel reflections which may be inclined. Radar facies 4 (RF4) is characterized by discontinuous to continuous oblique to curves

Fig. 4. Areal photographs of the onshore areas taken in Summer 1987 showing the location of data presented in this paper. Panel A shows Sandflugtdalen and the associated outlet glaciers of the Greenland Ice Sheet. Panel B shows the area near Mount Keglen which is located southwest of Panel A. Panel C shows the modern delta plain, Kangerlussuaq village and the location of the Watson Bridge. The summer melt conditions lead to flooding conditions on the modern delta (lowermost image).

Please cite this article in press as: Storms, J.E.A., et al., The Holocene sedimentary history of the Kangerlussuaq Fjord-valley fill, West Greenland, Quaternary Science Reviews (2012), doi:10.1016/j.quascirev.2011.12.014

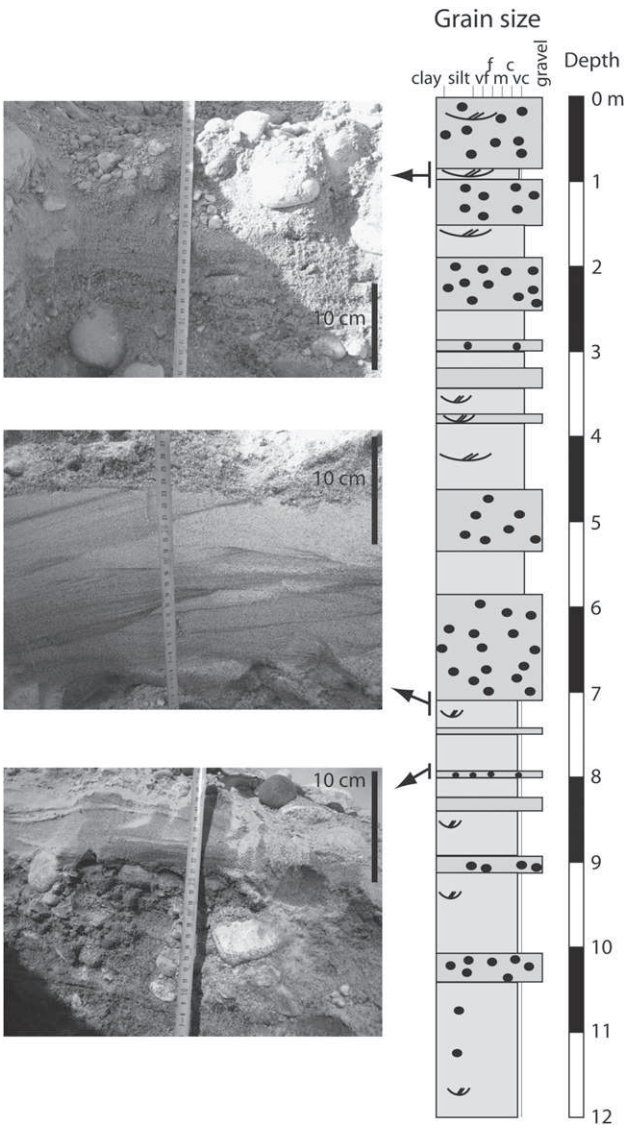

Fig. 5. Vertical section along a terrace intersection in Sandflugtdalen (for location see Fig. 4). The sequence consists of alternating well-sorted sand with cross bedding and heterogeneous beds consisting of pebbles, gravel and poorly sorted sand. Bed thickness range between 10 cm and 1.5 m. There is no evidence for cryoturbation or eolian activity. Photos show details of characteristic beds.

reflections. The inferred radar facies overly the bedrock that represents the base of the valley infill. This bedrock interface has been interpreted based on the lower boundary of overlying radar facies and specific reflection terminations such as onlap and downlap features. Below this bedrock interface reflection patterns have not been classified. Therefore, bedrock is not represented by a radar facies. The interpreted bedrock surface is correlated between all GPR images. Typically it will be easier to recognize the bedrock in a cross valley profile due to its typical U-shape than in a longitudinal profile. Correlation between the profiles ensures consistency in the interpretation. A similar approach has been applied in the correlation between the four radar facies.

5.1.3. Radar facies interpretation

The radar facies are used to classify typical reflection patterns which at a later stage were interpreted in terms of depositional environments. Based on published, observed and conceptual understanding of depositional environments in deglacial fjord settings and their associated stratigraphic response and position in the valley fill, we have interpreted the radar facies into three depositional environments (i) ice-contact (RF1), (ii) glaciolacustrine including a proximal (RF2) and distal modification (RF3), and (iii) glaciofluvial (RF4). These interpreted depositional environments enable us to reconstruct the valley infill history in relation to the ice-marginal setting.

5.1.3.1. Ice-contact deposits (RF1). Radar facies 1 shows a wide variety in reflections representing a range in depositional styles. The stratigraphic position of RF1 is an important criterion in the depositional environment interpretation as it occurs below radar facies 2, 3, and 4 while overlying the bedrock interface. This stratigraphic position infers that it is deposited prior to all other radar facies encountered in the GPR data. Combined with the presence of large clasts (inferred from diffractions (hyperbolas) patterns in RF1), we interpret RF1 as ice-contact deposits. Ice-contact deposits (IC) will represent a range of deposits units such as grounding-line fans, proglacial deltas, tills and moraines. In absence of sedimentological (core) data, these reflections cannot be classified in more detail.

5.1.3.2. Glaciolacustrine deposits (RF2 and 3). Radar facies 2 and 3 represent sediments that have been deposited predominantly by suspension fallout in a standing body of water (proglacial lake) generating continuous parallel reflections. The deposits show a gradient from proximal (inclined parallel reflections; GL-Pr) to distal (near-horizontal parallel reflections, GL-dis) settings relative to the palaeo ice margin.

5.1.3.3. Deltaic deposits (RF 4). Radar facies 4 is interpreted as deltaic deposits (D). The data show clear clinoform bottomsets and foresets indicating a progradational setting into a shallow body standing of water. Due to the technical GPR problem (mentioned in the Methods section) we were unable to image the topsets. Sedimentological evidence of the deltaic deposits (RF 4) is presented in Fig. 5. The strong grain size contrasts as described above will provide clear reflectors in the radar profile.

Fig. 6 shows three radar profiles and their interpretation. Line 20-74-72 shows a section of the longitudinal infill of Sandflugtdalen (for location see Fig. 7) of a subbasin bounded by bedrock sills. At the deepest part of the subbasin the infill is approximately 80 m thick. The infill shows distinct ice-contact deposits (IC) situated at the bedrock contact. The thick stack of ice-contact deposits lodged behind and on top of the bedrock sill in the western part of the profile formed a potential dam behind which a 1–1.5 km long and 50 m deep proglacial lake formed. An infill of up to 40 m distal glaciolacustrine deposits (GL-Dis) occurred as interpreted from the near-horizontal continuous parallel reflections (RF3; Table 2). A deformation feature (curved normal fault; listric) is present in the distal glaciolacustrine deposits. It is characterized by an offset of reflections that can be attributed to differential compaction above the irregular geometry of unit IC. Proximal glaciolacustrine deposits, characterized by less continuous reflections originating from higher energy conditions (RF2; Table 2) occur near the lake margin. Superimposed on the glaciolacustrine deposits are bottomsets and foresets of deltaic origin forming a thick progradational sequence. The overall thickness of this progradational sequence decreases from 30 m to 15 m in the west (including the 'no data' zone up to the present surface).

Line 80 (Fig. 6) shows a symmetrical U-shaped valley floor, with asymmetric ice-contact deposits which are up to 40 m thick. The ice-contact deposits show many hyperbolas indicating the presence of large boulders. Fig. 7 shows that line 80 is located in front of

Please cite this article in press as: Storms, J.E.A., et al., The Holocene sedimentary history of the Kangerlussuaq Fjord-valley fill, West Greenland, Quaternary Science Reviews (2012), doi:10.1016/j.quascirev.2011.12.014

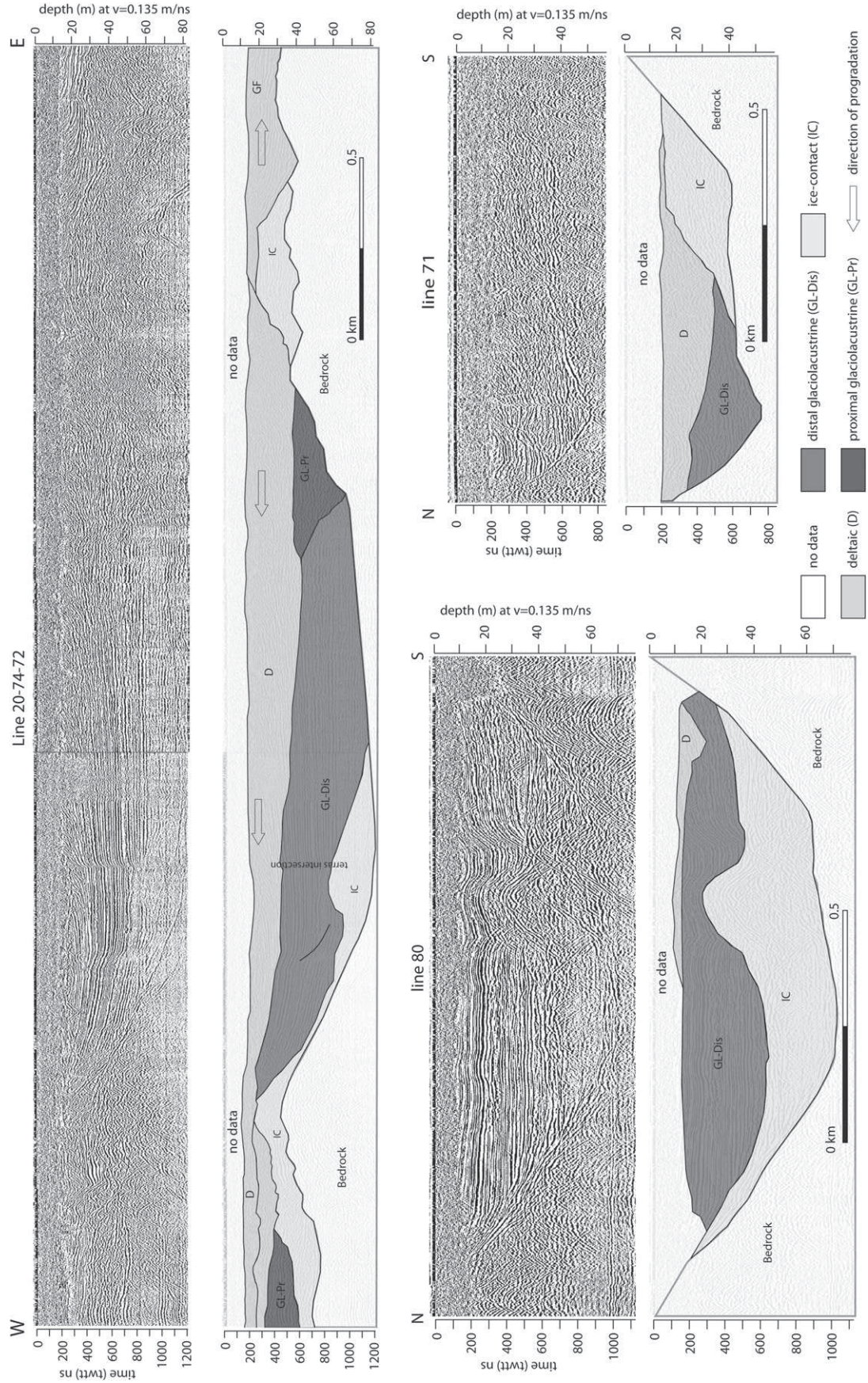

Fig. 6. Three GPR profiles (50 MHz) in Sandflugtdalen (for location see Fig. 7). The data were collected in Spring 2008 and show the stratigraphic pattern of a glacial valley infill. Line 20-74-72 represents a longitudinal section. This profile shows two additional features in the interpretation panel. The first is a vertical offset caused by a topographic feature. Here the radar crossed a terrace escarpment with near a vertical drop (from west to east) of approximately 8 m. Further to the west from the terrace intersection is a listric fault (indicated by the black curved line). This fault is present only in the distal glaciolacustrine deposits and may represent a growth fault. Lines 80 and 71 represent sections across the valley infill. Interpretation is based on radar facies (Table 2). The top section of the profiles only show noise due to technical problems. See text for further explanation of the sections.

Please cite this article in press as: Storms, J.E.A., et al., The Holocene sedimentary history of the Kangerlussuaq Fjord-valley fill, West Greenland, Quaternary Science Reviews (2012), doi:10.1016/j.quascirev.2011.12.014

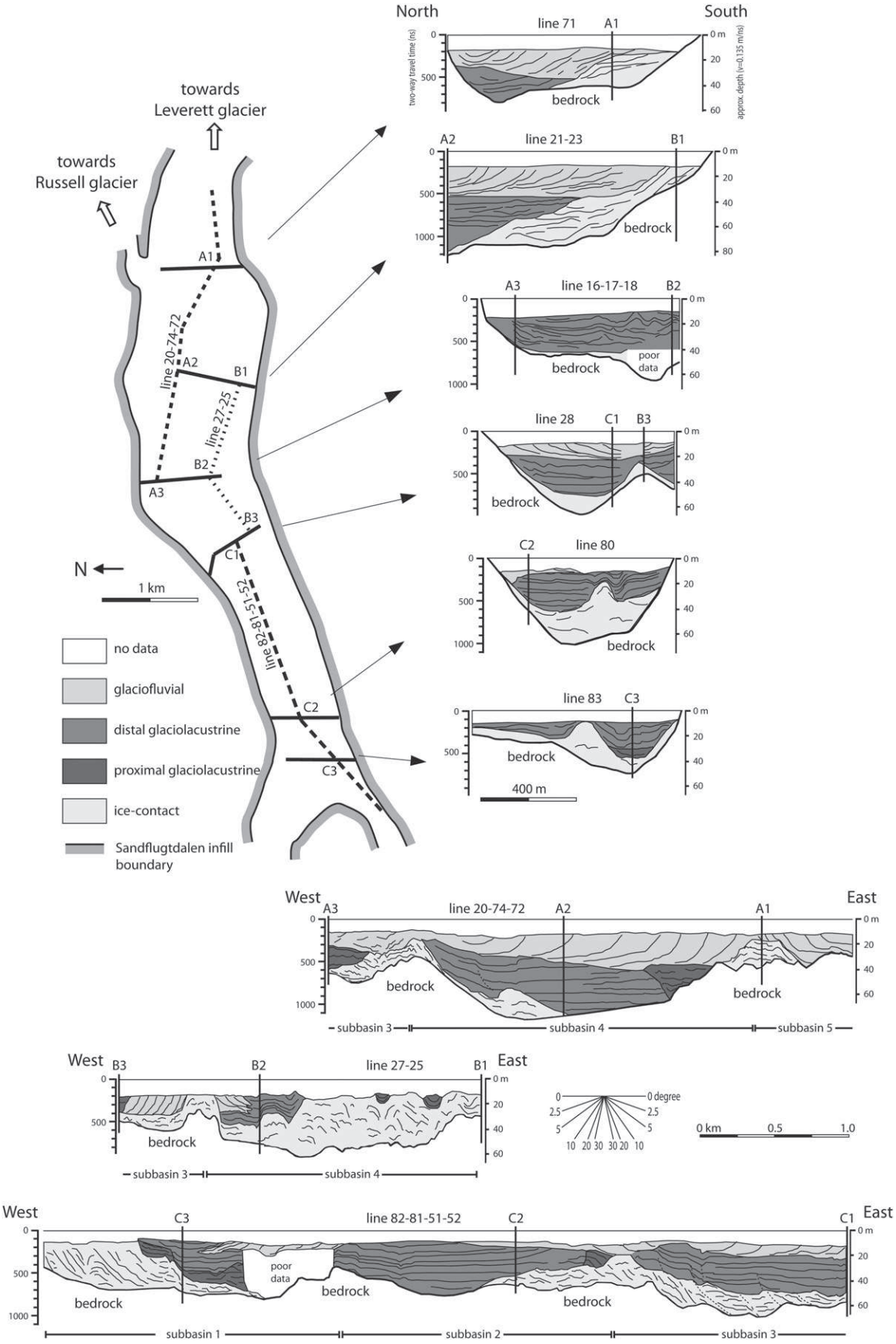

Please cite this article in press as: Storms, J.E.A., et al., The Holocene sedimentary history of the Kangerlussuaq Fjord-valley fill, West Greenland, Quaternary Science Reviews (2012), doi:10.1016/j.quascirev.2011.12.014

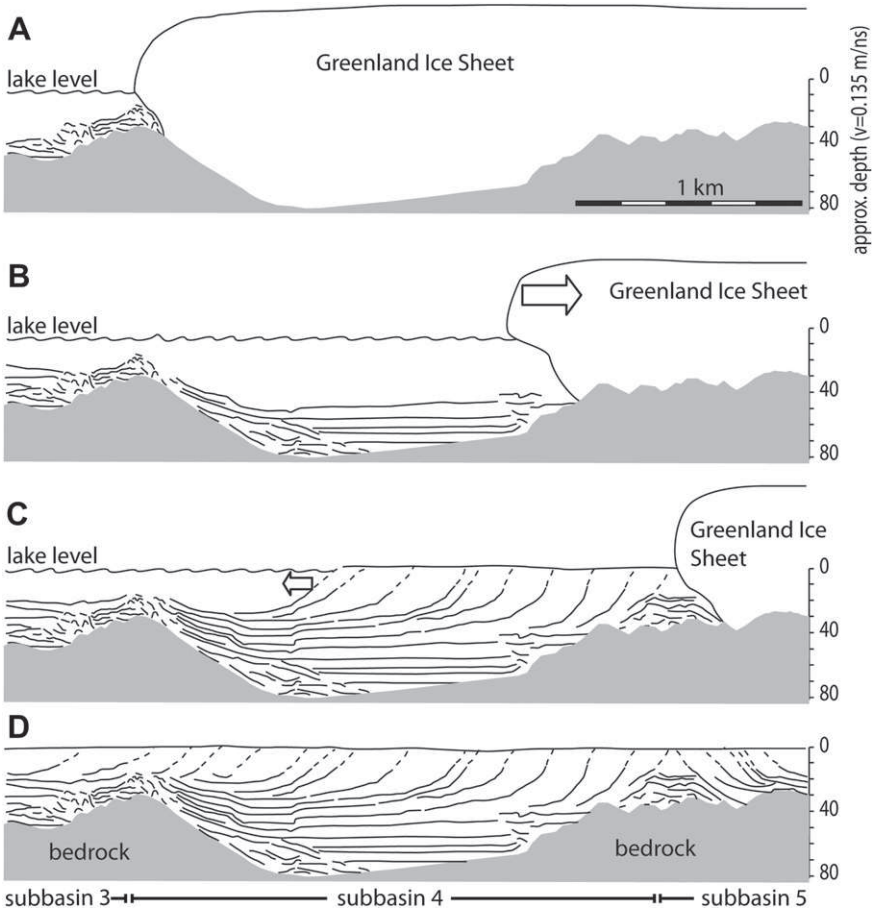

Fig. 8. Schematic reconstruction (A–D) of the infill of subbasin 4 (Sandflugtdalen, for location see Fig. 7) based on reflections in the radar profiles (50 MHz). Based on the position of ice-contact deposits at the bedrock sill, we interpret that the ice margin retreat temporarily paused near the sill which led to the deposition of the ice-contact deposits. The ice margin rapidly retreated across the deep part of the subbasins to the adjacent bedrock sill where it lingered again. The infill of the intermediate subbasin consists of glaciolacustrine to deltaic deposits.

a junction in the valley which were both occupied by glaciers. Therefore, the anomalous thickness of IC deposits in the middle of the profile may be related to moraine deposition at the divergence of the glacier into a northern and a southern branch. Overlying the ice-contact deposits are approximately 30 m of distal glaciolacustrine sediments. A thin sequence of deltaic (toeset) deposits in the south indicate that the deltaic deposits prograded in an approximately 10 m deep lake.

Valley basement depth is significantly less further to the east (line 71, Figs. 6 and 7). Here, ice-contact deposits flank the southern valley side, but are absent on the northern flank where glaciolacustrine deposits are overlain by deltaic deposits.

5.1.4. Reconstruction of the valley infill

Fig. 7 shows all interpreted radar profiles in Sandflugtdalen. The longitudinal profiles show that Sandflugtdalen can be subdivided into 5 subbasins which are all separated by bedrock sills with overlying ice-contact deposits. The depths of these subbasins range between 80 and 50 m (for subbasin 1–4). Line 27-25 shows that subbasin 4 has a clear increase in ice-contact deposits along its southern margin.

Line 20-74-72 shows a decreasing thickness trend in deltaic deposits toward the west. The thickness reduces from 35 m near intersection A1 (Fig. 7) to 20 m near the distal end of subbasin 4. Clinoform dip does not show a significant change along the 2 km progradation distance indicating that the sediment grain size transported by the fluvial system between the ice margin and the delta front may have been relatively constant. However, continuous and synchronous glaciolacustrine deposition in the distal parts of the proglacial lake led to a reduction in accommodation space which resulted in a decreasing thickness of the deltaic foresets.

Based on the interpreted GPR data of subbasin 4 we reconstructed the sedimentary history of the basin fill. The basin boundaries coincide with bedrock sills (Fig. 8A) where a significant ice-contact deposit is formed during a relative stable ice margin position. Subsequently, a vast amount of glaciolacustrine infill takes place. After the re-establishment of the ice margin at the adjacent sill (Fig. 8C), ice-contact deposits form with typical down- and

Fig. 7. Overview of all interpreted GPR profiles (50 MHz) in Sandflugtdalen. See Fig. 4A for the detailed morphology and the positions of Leverett and Russell glaciers. Cross sections of GPR profiles (e.g. A1) are indicated. Note that the horizontal scale differs for the north-south and east-west profiles. The north-south sections (lines 82-81-51-52, 27-25 and 20-74-72) show that Sandflugtdalen valley fill consists of 5 subbasins. Listric dotted black lines indicate listric faults with an offset in eastward direction (growth faults). The valley crossing profiles show non-symmetrical infill patterns with varying thicknesses of ice-contact, glaciolacustrine and deltaic deposits. Cross sections between longitudinal and perpendicular profiles are indicated by vertical lines with annotations (e.g. A1, C2).

Please cite this article in press as: Storms, J.E.A., et al., The Holocene sedimentary history of the Kangerlussuaq Fjord-valley fill, West Greenland, Quaternary Science Reviews (2012), doi:10.1016/j.quascirev.2011.12.014

upstream dipping structures (e.g. Powell, 1990; Lønne, 1995). As the proglacial lake depth rapidly decreases by continuous glaciolacustrine deposition, deltaic progradation is initiated forming steeply inclined clinoforms (>10°). The decreasing clinoform length (c.f. decreasing water depth) indicates that glaciolacustrine deposition proceeded down dip from the deltaic progradation (Fig. 8C). Eventually the complete basin is filled while the ice margin retreated further eastward. This retreat resulted in a decoupling of Russell and Leverett outlet glaciers. Although our data do not permit for a detailed reconstruction of this decoupling, we do see during this stage significant deltaic deposition with source in a northeastern direction (based on the combined apparent dip in Line 20-74-72 and 71).

5.1.5. Palaeo sedimentation rates

The presence of a series of infilled proglacial lakes discussed above has major implications for the timing of the infill. The final part of an infill is characterized by coarse grained deltaic sediments (Fig. 5). These sediments would not be available in case a proglacial lake had formed further upstream by ongoing ice margin retreat. Such a proglacial lake would capture all coarse grained (bedload) sediments to form ice-contact deposits while a significant volume of fine-grained (suspended) sediments will be captures in the proglacial lake as glaciolacustine deposits. Only a portion of the available fine-grained sediment released by the retreating ice margin would be able to escape the adjacent proglacial lake. Based on this, we therefor assume that the infill was (near) completed by the time the ice margin continued to retreat. This implies that Sandflugtdalen valley was already filled with sediment at the same time Ørkendalen regional moraine system was being formed (Fig. 2). The infill of Sandflugtdalen valley therefore is determined to have occurred between the formation of the Keglen and the Ørkendalen regional moraine systems, respectively 6496–7185 cal yr BP and 6406–7028 cal yr BP. Based on these partly overlapping ages, the infill of Sandflugtdalen occurred over a maximum period of approximately 800 years but presumably less. As we have insufficient time control to determine the timing of the five individual subbasins, we assume that the five subbasins (1–5) were filled sequentially and that their volumes are approximately similar. Based on these assumptions, the average time it took for a basin to fill was maximum 160 years. From the radar profiles we inferred an average thickness for the infill along the valley axis of 60 m, which leads an average minimum deposition rate of 0.38 m/y. Other studies that report deglaciation sedimentation rates indicate values as low as 0.034 m/y in Målselvdaln, Norway (Eilertsen et al., 2006) or as high as 13.0 m/y in Alaska (Powell and Molnia, 1989). Typical values on Spitsbergen are 0.1–0.25 m/y (Boulton, 1990; Elverhøi et al, 1983).

5.2. Keglen delta

Ten Brink and Weidick (1974) mentioned the presence of a delta (Keglen delta) landward of Watson Bridge that formed during the period that the GIS margin lingered near Mount Keglen (forming the Keglen moraine system at 6496–7185 cal y BP). In addition to the sedimentary infill of proglacial lakes at Sandflugtdalen, this delta forms a main depocenter, which shows evidence of direct marine (open fjord) influence (Ten Brink and Weidick, 1974).

5.2.1. Data

New GPR data between Mount Keglen and Watson Bridge indicate a shallow bedrock depth, which combined with the limited valley width (50 m and 1 km near respectively Mount Keglen and the Golf course) results in limited accommodation space for Keglen delta. Based on topographic data and GPS measurements, the elevation of the Keglen delta flood plain ranges from +80 m near the waterfall to +57 m (radar line 90; Fig. 9). The latter is the top of the progradational delta plain. Further downstream, we described a vertical section exposed along a terrace escarpment with top surface at +28 m above present sea level (log 87, see Fig. 10). The top of the section shows bedding structures with graded beds that include pebbles and coarse sand in the upper part. No evidence of channelized flow was found in this section. The lower part consists of alternating fine sand and silt. Two shells at +26 m and +13 m above mean sea level enclosed in respectively deltaic and the underlying marine deposits have been dated to respectively 6425–6657 and 6669–6916 cal y BP (Curl-10988 and Curl-10986; see Table 1).

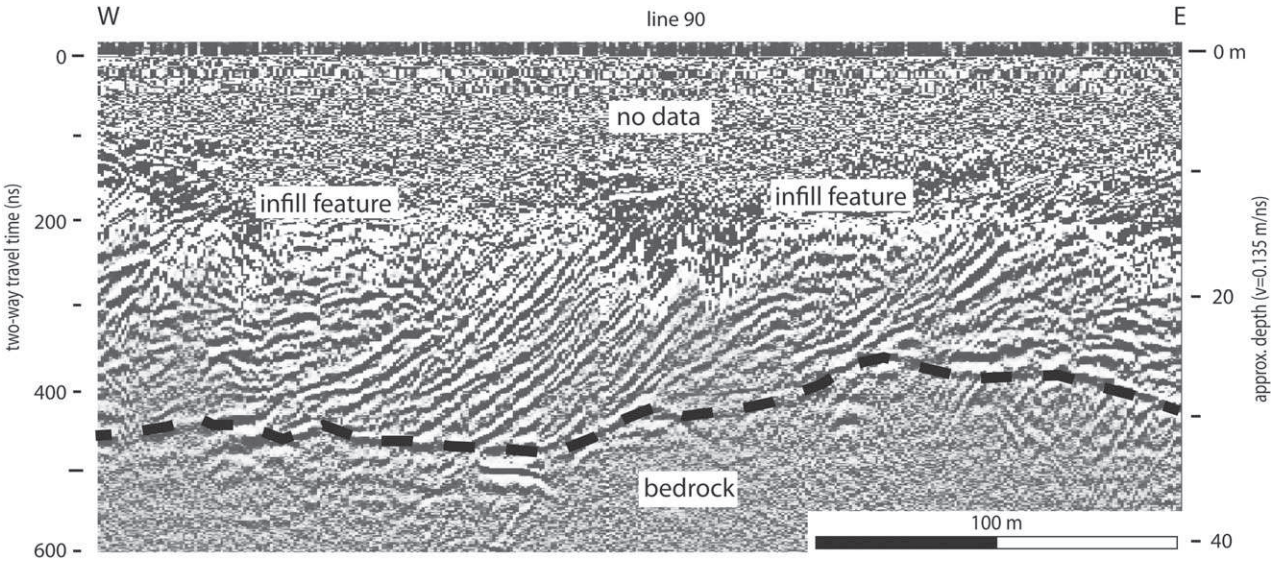

Fig. 9. Example of GPR data (50 MHz) showing the Keglen Delta, west of the confluence of Sandflugtdalen and Ørkendalen valley, prograding over bedrock (black dotted line between 30 and 35 m depth). For location see Fig. 4C. The clinoforms are irregular and show infill features (indicated in the figure) which may be related to a prograding river efflux position. The data of the top section are obscured by technical problems. The absence of glaciolacustrine or glaciomarine deposits underlying the prograding Keglen delta indicates a low accommodation space at this specific site and high energetic depositional system.

Please cite this article in press as: Storms, J.E.A., et al., The Holocene sedimentary history of the Kangerlussuaq Fjord-valley fill, West Greenland, Quaternary Science Reviews (2012), doi:10.1016/j.quascirev.2011.12.014

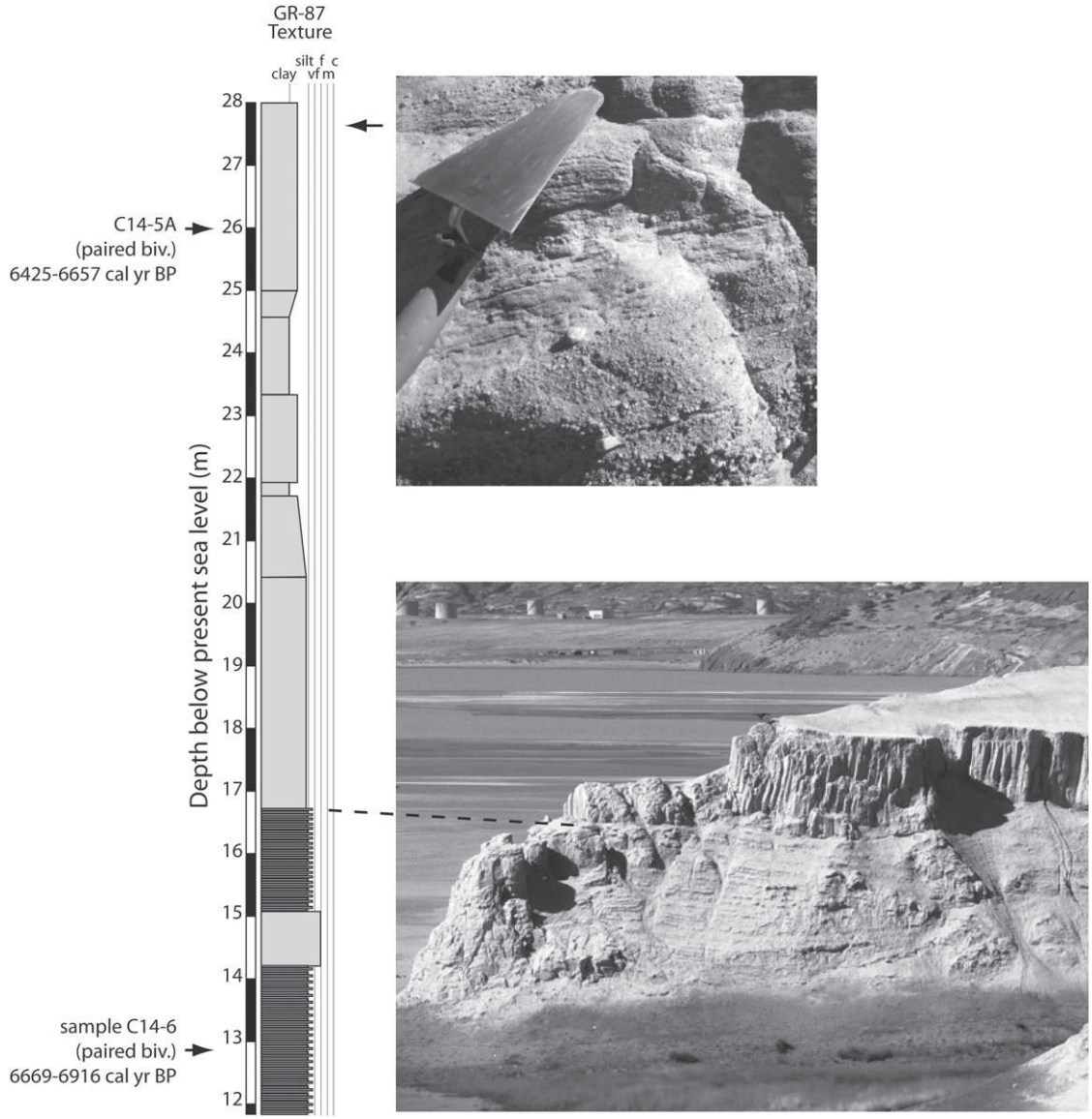

Fig. 10. Vertical section of the marine terraces near Kangerlussuaq airport (for location see Fig. 4C) with photo panels showing details of the exposed terrace in the distal part of the prograding Keglen delta. The vertical section consists of finely laminated glaciomarine prodelta sediments which are overlain by shallowing-up delta front deposits which are more homogeneous. Yet, due to a decrease in the supply of coarse grained these proximal deposits are finer grained than the more distal prodelta sediments. Two samples (shells) for radiocarbon dating have been collected from this vertical section which indicates a formation synchronous to the formation of Keglen moraine system.

Further southwestward, approximately 1.7 km downstream of Watson Bridge and flanking the northern margin of the modern delta, our field data shows no evidence of deltaic deposition associated to the Keglen delta. Here, laminated silt deposits suggest deposition in a distal marine setting (Fig. 10).

Three onshore seismic profiles west of Watson Bridge show a rapid increasing sediment thickness toward the west (Fig. 11) from approximately 70 m (spread 4) to 300 m (spread 5) to 370 m (spread 6). The seismic data show no internal reflection patterns due to the limited acoustic contrasts within the delta sediments.

5.2.2. Interpretation

Keglen delta formed during a fast sea level fall of approximately 26 mm/y (Fig. 3). The limited accommodation space in combination with the falling sea level allowed for a very fast progradation of the coastline. As the ice margin continued to retreat into Sandflugtdalen the formation and subsequent infill of proglacial subbasins will have significantly limited the bedload component of Watson River. However, we lack data on the valley infill history of the adjacent Ørkendalen and how this affected the formation of the Keglen delta. Log 87 (Fig. 10) represents a shallowing depositional succession, ranging from glaciomarine (possibly prodelta) to delta front. The water depth during deposition is not clear as delta plain deposits are absent.

We presume the +57 m delta plain level (Fig. 9) to be a palaeo sea level indicator. This suggests the time of formation was approximately 7100 cal y BP (inferred from Fig. 3) which is synchronous with the formation of the Keglen moraine system (Ten Brink and Weidick, 1974). The dated shells in Log 87 indicate that deltaic deposition continued for at least 500 years (Curl-10988, 6425–6657 cal y BP, see Table 1). As the delta entered the open Kangerlussuaq Fjord seaward of Watson Bridge the rate of progradation decreased rapidly due to the vast increase in bedrock depth (Fig. 11) (Muto and Steel, 1992).

Please cite this article in press as: Storms, J.E.A., et al., The Holocene sedimentary history of the Kangerlussuaq Fjord-valley fill, West Greenland, Quaternary Science Reviews (2012), doi:10.1016/j.quascirev.2011.12.014

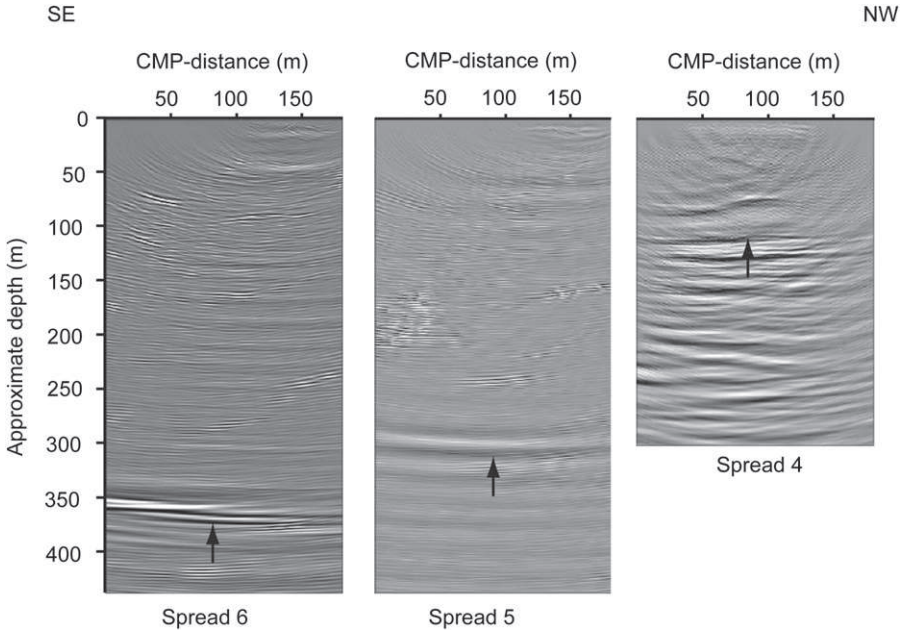

Fig. 11. Time migrated, depth converted reflection seismic images at the modern delta (for location see Fig. 4C) showing a gradual southwestward increase of valley infill thickness. The interpreted bedrock reflection is indicated with an arrow. No internal reflections of the valley infill are imaged. Approximate depth are obtained with a seismic velocity of 2000 m/s.

The fast sea level fall during the formation of Keglen delta resulted in a segmented flood and delta plain characterized by terraces. This makes it difficult to correlate terrace levels over longer distances at the field site. Fig. 12 shows examples of preserved flood plain terraces associated with the progradation of Keglen delta.

5.3. Modern delta including Kangerlussuaq Fjord

5.3.1. Core data and radiocarbon dates

Eight sediment cores have been retrieved from the fjord seafloor during the GIMEXMAR'92 cruise, which have been described by Bakker (1996). Recently nine new radiocarbon dates have been analyzed from shell fragments in these sediment cores which are shown in Fig. 13 (see also Table 1). Core A, located along the flank of the Sarfartôq sill, is dominated by sediments from the Sarfartôq drainage system. Cores B to G are aligned from distal to proximal relative to the Watson River mouth. All six cores show alternations of sand and clay (except for core E which is located in the Angujârtorfik side valley). The thickness of individual sand layers varies between a few centimeters to 3 m.

5.3.2. Interpretation of offshore sedimentation rates

The sedimentation rate for core D is based on a calibrated radiocarbon date derived from a shell fragment and averages 2.0–2.2 cm/y. The radiocarbon datings in cores B and F are modern (<250 years old based on the reservoir age of the fjord water). For core B this would indicate that a sediment thickness of 8.06 m has been accumulated in less than 250 years resulting in a minimum sedimentation rate of 3.2 cm/y at this distal location.

5.3.3. Geophysical data

Existing seismic data (Larsen, 1977; Fig. 13C) show that the total sediment thickness between Sarfartôq sill and the Angujârtorfik side valley is about 350 m. Our seismic boomer data only image the upper 75–125 m of this infill (Fig. 13D). In total, 244 km of seismic boomer data were collected between the Fjord entrance and the present-day delta front the Watson River. We will focus on a profile that runs parallel to the fjord from the Sarfartôq sill to approximately 1 km west of the mouth of the Watson River delta (Fig. 13).

Water depth gradually increases between the modern delta front in the southwest and the emerging bedrock sill affects the water depth (Fig. 13A). The maximum slope of the delta front is about 1.5° (gradient of 0.026) which is quite subtle. The proximal reflections (near the modern delta) are undulating and show small-scale on- and offlap features and crosscutting relations. A number of reflections are continuous for over >5 km while others are very discontinuous. Further southwestward (near core G), the gradient of the reflections decreases while near core F these reflections become very continuous and near parallel.

An important reflection (Reflection A) is mapped along the full length of the profile (annotated in Fig. 13A) which shows a shift in reflection style. In the northeast, this reflection forms the base of a large scale downlap that represents the progradation of the modern delta. The shift in dip direction toward the northeast results from differential compaction caused by the progradational overlying delta.

The seismic boomer data show numerous subaqueous, erosional channels cut into parallel stratified delta front deposits. These channels can be grouped into two types. Type one is flanked by asymmetric subaqueous levee systems (2 channels observed, Fig. 14A) while type two is erosional, i.e. an entirely negative landform (12 channels observed). The levees at both sides of the channel are about 10 m high and consist of parallel wavy reflections. The erosional channels cut deep (up to 30 m) in pre-existing stratigraphy (Fig. 14B) and have very steep channel margins. Most erosional channels occur in the northeast, where the basin floor slope is relatively steep (between 0.5 and 1.0°). The widths of the channels cannot be determined because of the unknown orientation of the channel. Since the majority of the seismic boomer data is oriented down depositional dip, we may assume that the channel system is meandering and therefore individual channels may be imaged several times. The number of individual channel systems is unclear and cannot be extracted from the 2D seismic lines.

Assuming a conservative sedimentation rate of 3.2 cm/y (based on the minimum sedimentation rate of Core B, Fig. 13), the

Please cite this article in press as: Storms, J.E.A., et al., The Holocene sedimentary history of the Kangerlussuaq Fjord-valley fill, West Greenland, Quaternary Science Reviews (2012), doi:10.1016/j.quascirev.2011.12.014

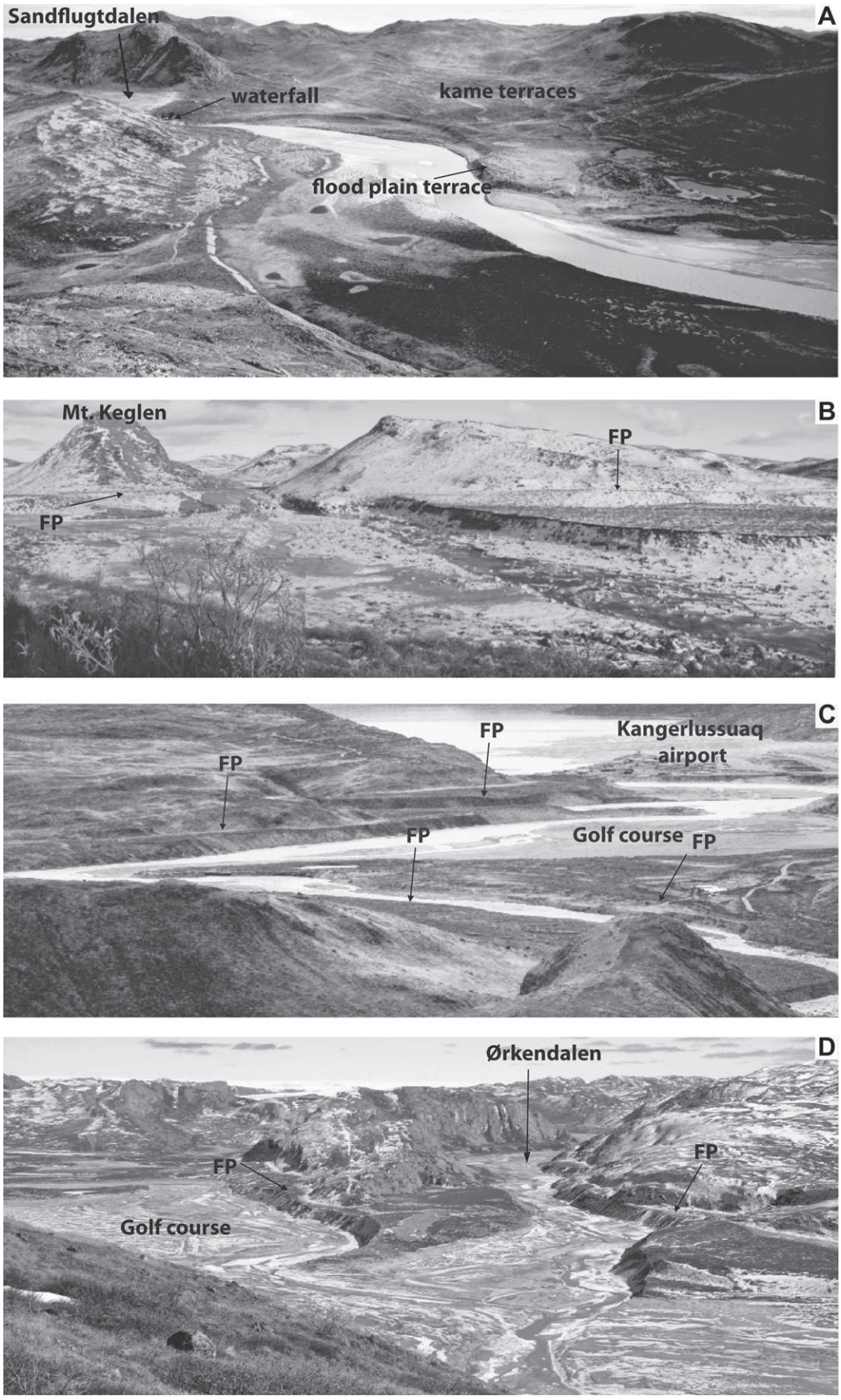

Fig. 12. Photo panels showing the top section (terraces) of Keglen delta flood plains downstream of Sandflugtdalen. For location and orientation of the photo panels see Fig. 4B. While the GIS margin was located near the waterfall (panel A) a regional moraine system formed (Keglen moraine system). At the same time a rapidly prograding fluvial system formed which consisted of dissected flood plains (FP) near Mount Keglen (panel A–D) and a prograding delta near Watson Bridge (see Fig. 9).

Please cite this article in press as: Storms, J.E.A., et al., The Holocene sedimentary history of the Kangerlussuaq Fjord-valley fill, West Greenland, Quaternary Science Reviews (2012), doi:10.1016/j.quascirev.2011.12.014

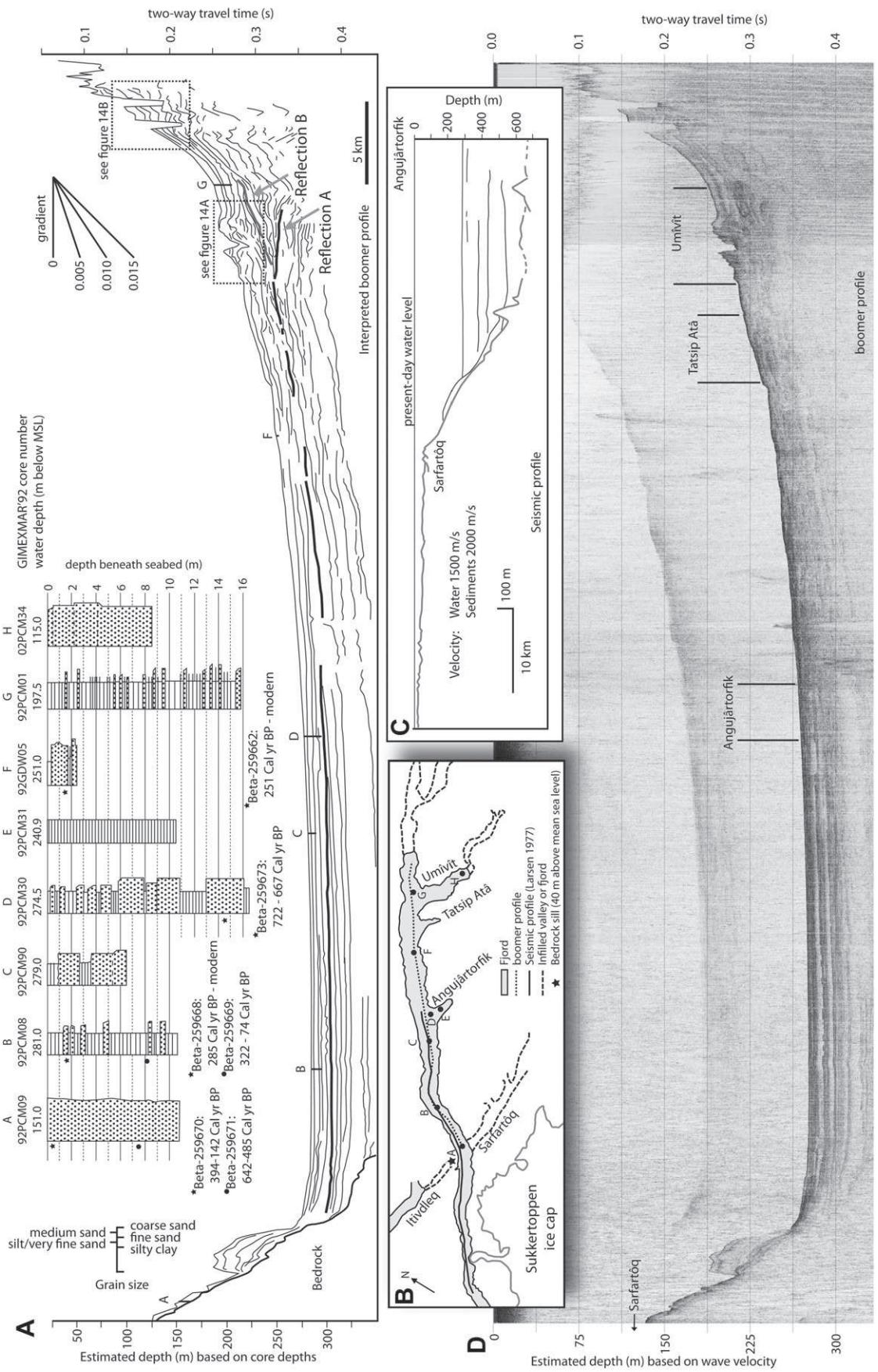

Fig. 13. Seismic boomer data (D-lower panel) with interpretation (A-upper panel) from Kangerlussuaq Fjord. Location of the seismic section is shown in the left middle panel (B). An older seismic section from Larsen (1977) is shown in the right middle panel (C). Eight cores, taken during the GIMEXMAR'92 cruise (1992) illustrate the heterogeneous sediments consisting predominantly of alternating sand and clay layers varying in thickness between millimeter and meter scale. The seismic data from Larsen (1977) reveal that Kangerlussuaq Fjord is over 600 m deep and filled with nearly 400 m of sediment in the distal sections (between Sarfartôq and Angujârtorfik). Reflections of the boomer seismic data reveal detail sedimentary architecture of the upper 100 m of the infill. Here the distal portion of the infill is a low energy deposit with parallel, horizontal reflections. Core data show that sand is deposited in individual layers which may be associated with turbidity currents originating from large melt water floods or jökulhlaups. Clinoforms can be seen in the proximal sections of the Watson River efflux. The irregular nature of these clinoforms is interpreted to represent the effects of turbidity flows and mass movements. Distinct channels are visible in this proximal section of the profile (Fig. 14). See text for further explanation.

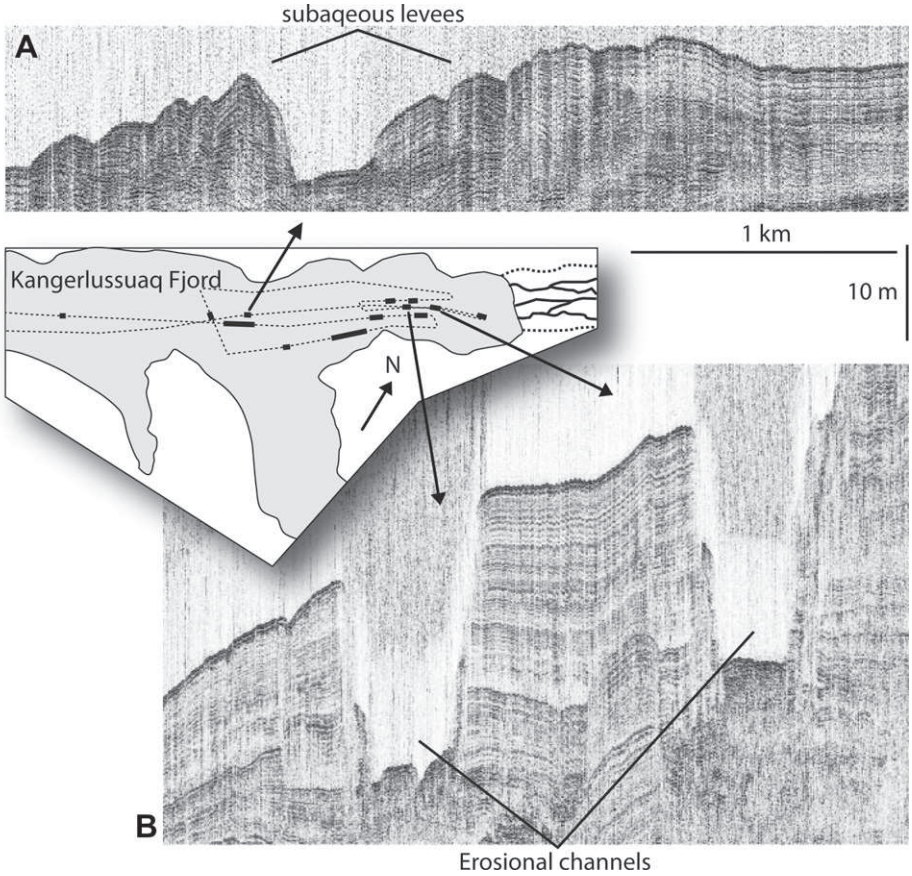

Fig. 14. Detailed section of the seismic boomer data showing two channel types. Erosional channels, up to 30 m deep, are seen in the upper part of the prograding Watson delta while channel morphology changes in deeper water. Here subaqueous levees are formed while the channels are less deep. In total 13 channels have been identified of which only two show a levee system. We presume that the channel system links to the Watson River efflux.

sediments at the base of the erosional channel (approximately 30 m below the seafloor) are about 900 years old. This, provides a maximum age estimate for the subaqueous channel.

5.3.4. Geophysical data interpretation

The inner part of Kangerlussuaq Fjord, east of Sarfartôq (Fig. 13B) is a closed sediment sink. Sediment input originates from four glacial melt water systems, the Sandflugtdalen/Ørkendalen (Watson) system discussed above, as well as the Umîvît, Tatsip Atâ, and Angujârtorfik drainage systems. At present the latter two systems produce little sediment because they are decoupled from the GIS (Oele, 1992).

The seismic reflection configuration shows a shift in depositional pattern from a proximal delta front in the northeast of the fjord to distal marine deposits in the deepest section of the fjord. Reflection A marks a shift in proximal depositional style which can be traced throughout the fjord infill. Based on the radiocarbon date in core D (Beta-259673; see Table 2) we can infer that sediments overlying Reflection A (located a few meters below the dated shell sample) are associated with a deposition during sea level rise (inferred from Fig. 3). Progradation rate of the prodelta and delta front would have decreased and eventually stopped between approximately 1500 and 1000 years BP as accommodation space was created at the modern delta plain due to sea level rise. The toe sets between Reflection A and Reflection B (Fig. 13A) represent this final progradation phase. Deposits overlying Reflection B are characterized by parallel reflections indicating that depositional style is more dominated by suspension fallout.

As the overall progradation of the modern delta halted the effects of potential hyperpycnal flows linked to jökulhlaups generated along the ice margin (Russell, 2007, 2009) became more significant. Hyperpycnal flows can generate turbidity currents which are erosional at high gradient slopes and depositional when the gradient decreases (Kneller, 2003). Erosion caused by these subbottom flows is most effective where the delta front is steepest (see Fig. 14B) leading to the formation of deep erosional channels. Further seawards, subaqueous levees are formed along these channels (Fig. 14B). Characteristics of lobe formation (undulating reflections) are seen in the area near Core F. These lobes are most likely associated with the sand-rich layers as encountered in the sediment cores, similar to descriptions by Ó Cofaigh et al. (2001), Desloges et al. (2002) and Prior et al. (1986).

It is not clear whether the formation of the observed subaqueous channels is governed by the decrease in progradation rate or an increase in jökulhlaup frequency. Foreman et al. (2007) state that the GIS margin for the Neoglacial, the LIA and the present-day all occur with 2 km. These latter processes may have increased the jökulhlaup frequency leading to an increase of hyperpycnal flow events. Furthermore, the timing may also coincide with the end of the medieval warm period and the onset of the Little Ice Age (LIA). Moraines near the present-day ice margin of Russell and Leverett glaciers have been linked to the LIA (Van Tatenhove et al., 1996). Although local palaeoclimate and palaeoecological studies (Eisner et al., 1995; Willemse and Törnqvist, 1999; McGowan et al., 2003) show no indications for major changes climatic changes over the last 1000 years, local ice advance may lead to abrupt hydrological changes and the formation of ice-marginal lakes (Knight et al., 2000).

Please cite this article in press as: Storms, J.E.A., et al., The Holocene sedimentary history of the Kangerlussuaq Fjord-valley fill, West Greenland, Quaternary Science Reviews (2012), doi:10.1016/j.quascirev.2011.12.014

6. Holocene sedimentation history

Based on the depositional development presented above we have constructed a chronostratigraphic diagram (Fig. 15) that summarizes the Holocene sedimentation history Kangerlussuaq Fjord and valley infill. We have synthesized three main depositional phases:

6.1. Phase I: >7000 cal year BP

Phase I is characterized by deposition in Kangerlussuaq Fjord. The ice margin is represented by a tide-water glacier given the extensive fjord depth westward of Watson Bridge. The valley east of the current Watson Bridge is still glaciated.

6.2. Phase II: 7000–1500 cal years BP

Phase II is characterized by a significant change in depositional style. The ice margin retreats from Kangerlussuaq Fjord into the valley and becomes a land-based glacier. The formation of Keglen delta and the infill of the subbasins at Sandflugtdalen represent major depositional events in the first part of phase II. Keglen delta and the associated offshore sediments represent marine deposition while simultaneously Sandflugtdalen is represented by the back-stepping infill of at least five subbasins. The latter has led to strong eolian activity directly following the infill of subbasins (Dijkmans and Törnqvist, 1991; Eisner et al., 1995; Willemse et al., 2003).

After the rapid progradation rate of Keglen delta has decreased, deposition continued in Kangerlussuaq Fjord with prodelta and delta front sediments derived from the Watson River. Due to ongoing relative sea level fall (Fig. 3), significant reworking and sediment bypass occurred between the land-based GIS margin and the progradational river mouth to the southwest. The prograding delta led to a forced regressive sediment body, similar to observations described by Corner (2006).

The previously deglaciated area which is presently covered by the Neoglacial GIS margin protrusion is not studied and provides an uncertainty in the depositional reconstruction. It is unclear how far the GIS margin retreated beyond its present-day position and how this affected deposition. Also there is uncertainty if and how the advancing GIS margin after 4000 cal y BP affected the coastline position resulting from possible changes in the sediment load of Watson River.

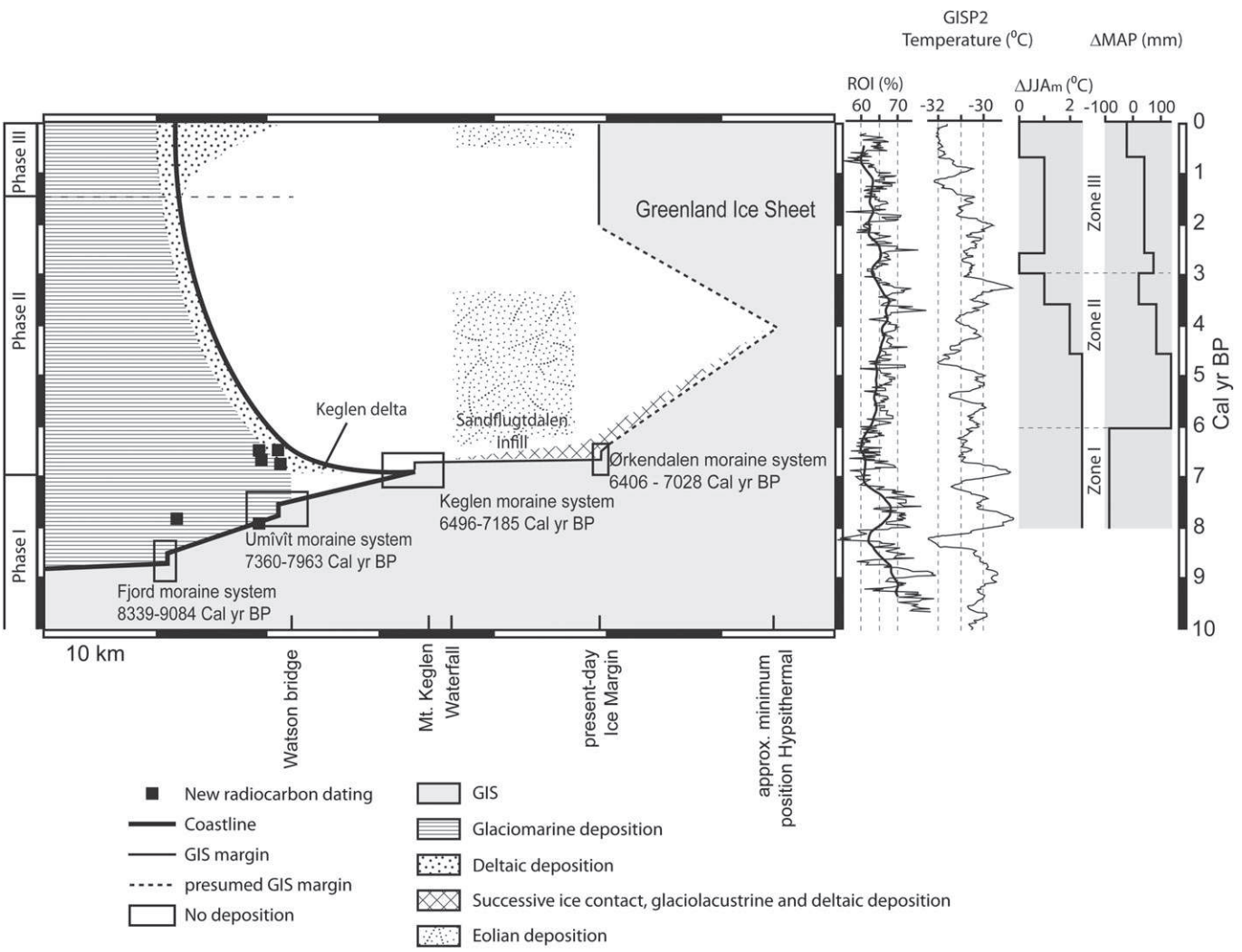

Fig. 15. Diagram summarizing the Holocene development of Kangerlussuaq Fjord and inland valleys based on previous studies and the presented data. Three phases of deposition are indicated. On the right-hand side four paleoclimate curves are shown based on three independent sources. The left curve shows the 'Residue On Ignition' for lake sediments (Willemse and Törnqvist, 1999) approximately 50 km west of Watson Bridge. The second curve shows the temperature based on oxygen isotope variation in the GISP2 core (Alley, 2000) while the two curves on the right-hand side represent the deviation of the June–July–August mean monthly temperature and the deviation of the Mean Annual Precipitation relative to the present-day situation (Aebly and Fritz, 2009) for lakes near Sandflugtdalen. See text for further explanation.

Please cite this article in press as: Storms, J.E.A., et al., The Holocene sedimentary history of the Kangerlussuaq Fjord-valley fill, West Greenland, Quaternary Science Reviews (2012), doi:10.1016/j.quascirev.2011.12.014

6.3. Phase III: 1500 cal years BP – present

During phase III deposition is restricted to the present-day delta and Kangerlussuaq Fjord while the area between Watson Bridge and the GIS margin is a sediment bypass zone. The depositional regime at the modern delta changes from progradational under sea level fall conditions to progradational under sea level rise conditions (Fig. 3). A delta plain is formed characterized by an aggrading delta plain with numerous small channels (Fig. 4). Surface sediments are better sorted than in Sandflugtdalen and pebbles are rare. There is no terrace formation at the present-day delta plain which is indicative for aggrading conditions at the delta plain as sea level rises during this phase (Fig. 3).

Offshore, subaqueous channels are formed during phase III while the rate of progradation of the modern delta decreases. The inferred age of these channels (see Section 5.3.1) is less than 1000 years. An increase in jökulhlaup frequency and associated hyperpycnal flows related to climatically induced variation of the GIS margin may have affected their formation.

7. Discussion

This study integrates a wide range of new and published data in order to construct a scenario of the deglacial sedimentary history of Kangerlussuaq. Validating this sedimentary history is presently challenging due to the lack of detailed time control and core data. Although a number of new radiocarbon dates have proved to be very valuable, the timing of formation of terraces and aggradation rates of flood and delta plains has not been resolved.

7.1. Kangerlussuaq Fjord blockage?

A bedrock sill, presently at +40 m above sea level separates Itivdleq fjord from Kangerlussuaq Fjord (Fig. 13B). The sill shows clear indications of channelized incision caused by flowing water (Sugden, 1972). Based on Ten Brink's (1974) emergence curve for the Sarfartôq and Itivdleq area the sill will have emerged above sea level between 7421 and 7719 cal years BP years ago (based on the radiocarbon sample K-1579 in Ten Brink, 1974), when the area was already deglaciated (Ten Brink and Weidick, 1974). This implies that both fjords were hydrologically independent after this time.

Given the small catchment area for the isolated Itivdleq fjord, this would imply that the fjord sedimentation rate should have decreased abruptly after 7421–7719 cal years BP. Radiocarbon dates of shells samples retrieved from cores at 138 and 367 m water depth at the inner Itivdleq fjord (Van der Meer et al., 1994) indicate that the youngest shells found in the cores are dated approximately 4000 years BP. Van der Meer et al. (1993) explain this by assuming that an emerging glacier from Sukkertoppen ice cap blocked Kangerlussuaq Fjord and raised the water level of the inner fjord by approximately 40 m. This would allow water and sediment to be spilled over the bedrock sill thereby rejuvenating sedimentation in Itivdleq fjord. A hypothesized water level rise of 40 m in Kangerlussuaq Fjord is however not supported by our observations from Keglen delta.

7.2. Palaeoclimate trends

A number of studies (e.g. Willemse and Törnqvist, 1999; Alley, 2000; Aebly and Fritz, 2009) have identified trends in the Kangerlussuaq palaeoclimate based on various proxies (Fig. 15). The Holocene thermal maximum (McGowan et al., 2003; Kaufman et al., 2004) continued in the Kangerlussuaq area until approximately 4000 cal y BP (Willemse and Törnqvist, 1999). A decreasing summer temperature was reported by Aebly and Fritz (2009) which gradually decreases from +2.5 to 0 °C between 6070 and 2600 cal y BP. This coincides with an overall decreasing mean annual precipitation (Fig. 15).

A retreating ice margin will release vast amounts of sediments (e.g. Hallet et al., 1996). As such, the proglacial sedimentary system will be affected by any climate induced GIS margin dynamics. De Winter et al. (in press) showed using numerical modeling that sediment delivery from the retreating ice margin exhibits a distinct time lag of several thousand years behind melt water flux. Therefore, the timing of the sediment released to and transported by the sedimentary system is not necessarily in phase with the climate induces GIS margin retreat.

While the regional response of the GIS on palaeoclimate is recorded by the documented regional moraine systems, the local sedimentary response in Kangerlussuaq is still unclear. As presented above, local depositional response in Kangerlussuaq Fjord is characterized by local depocenters, depocenter shift and sediment bypass. This is to a large extent governed by accommodation space which is reflected in the local morphology and the location of the GIS margin (Fig. 15). In Sandflugtdalen (landward of the marine limit), the depositional pattern is backstepping while its downstream time equivalent at Keglen delta is characterized by a forced regression. In both cases deposition is characterized by a rapid lateral depocenter shift while the vertical sediment thickness is limited. Identifying the sedimentary response to palaeoclimate change in such sedimentary records is therefore extremely difficult. Further downstream, in Kangerlussuaq Fjord, we expect a more complete vertical sedimentary record (Fig. 13) which may contain a palaeoclimate signal in terms of sedimentation rate or grain size. Yet our data lacks a detailed vertical age model and grain-size record.

7.3. Distribution of sediments

Fig. 16 shows the distribution of sediments in Kangerlussuaq Fjord based on new and existing data. It becomes clear that the

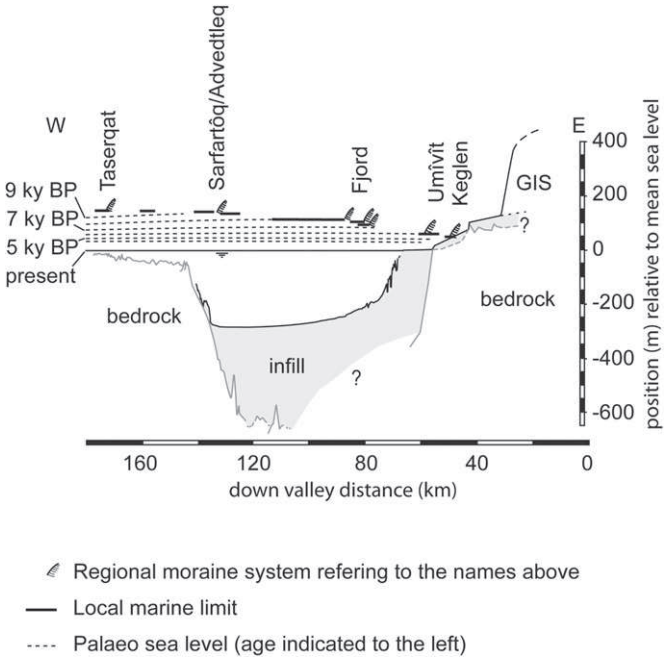

Fig. 16. Overview of the sediment distribution in Kangerlussuaq Fjord and inland valley fill based on seismic data from Larsen (1977) and data presented in this study. Indicated are the regional moraine systems as mapped by Ten Brink and Weidick (1974) and the location of the marine limit along the fjord (Weidick, 1993). The black doted horizontal lines show the palaeo sea level at the indicated ages (to the left).

Please cite this article in press as: Storms, J.E.A., et al., The Holocene sedimentary history of the Kangerlussuaq Fjord-valley fill, West Greenland, Quaternary Science Reviews (2012), doi:10.1016/j.quascirev.2011.12.014

majority of the sediment volume is situated in the deepest part of the basin between Watson Bridge and the bedrock sill near Sarfartôq. The majority of this infill is therefore younger than the Sarfartôq regional moraine system (8896–9727 cal y BP). Older sediments can be expected in Itivdleq fjord. Accommodation space in Kangerlussuaq Fjord westward of Sarfartôq valley is limited (Fig. 13C) and decreases in time as relative sea level falls (Fig. 16). Here tidal currents are relatively strong (Oele, 1992) due to the limited water depth resulting in resuspension and transport of sediments. As a result, no significant sediment accumulation occurred in the shallow section of the fjord westward of Sarfartôq (Fig. 13C). Furthermore, the boomer seismic data show no evidence of significant sediment transport from Sarfartôq valley in eastward direction by means of tidal currents (Fig. 13A).

8. Conclusions

The goals of this research were (1) to understand the fjord infill as a function of glacier fluctuations, sea level change and shifts in depocenter through time, (2) to reconstruct local deposition rates, (3) to characterize the fjord infill and to link on- and offshore data, and (4) to understand the effect of neoglacial ice readvance on the depositional system. The main conclusions are:

Kangerlussuaq Fjord infill and associated landward basin fill represent a continuous sedimentary system that can be linked to the deglacial history of the Greenland Ice Sheet with rapidly migrating depocenters. Three depositional phases have been identified. Phase I (>7000 years BP) represents glaciomarine deposition in Kangerlussuaq Fjord. Phase II (7000–1500 years BP) is characterized by the formation of Keglen delta and the rapid infill of the subbasins in Sandflugtdalen. The second part of Phase II is represented by sediment bypass onshore and ongoing sedimentation in Kangerlussuaq Fjord. Phase III (<1500 years BP) is characterized by a relative sea level rise and infilling of the modern delta plain and subaqueous channel formation at the delta front.

A large marine delta system (Keglen delta) formed synchronously with the formation of Keglen regional moraine system. Progradation rate decreased significantly when proglacial lakes formed landward which captured most of the sediment from the melt water streams. Ground penetrating radar of the valley infill in Sandflugtdalen show that at least five separate proglacial palaeo-lakes have existed that represent subbasins of 40–80 m deep which are separated by bedrock sills and overlying ice-contact deposits. The infills of the subbasins consist of ice-contact deposits overlain by glaciolacustrine deposits. The final stage of infill is represented by deltaic progradation. Radar data suggest that each proglacial palaeo-lake was filled subsequently while the overall retreating GIS margin halted temporarily at bedrock sills separating the subbasins.

Previously published seismic data show a 350 m thick sedimentary unit in the marine part of Kangerlussuaq Fjord. Cores show alternating clay and sand beds throughout the fjord infill in the upper 5–10 m. New high-resolution seismic boomer data show that the upper 75–125 m of this infill shows distal to proximal delta deposits. Subaqueous channels are present at the present-day seafloor which are related to the diminished progradation rate during the past 1000 years as sea level rose. Channels and lobes are formed by hyperpycnal flows associated with jökulhlaup events. It is not evident if jökulhlaup frequency has increased over this period.

We see no indication for a blockage of Kangerlussuaq Fjord caused by an advancing glacier form Sukkertoppen ice sheet around 4000 years BP.

Sedimentation rates associated with the Sandflugtdalen valley infill can be as high as ~0.38 m/y during rapid retreating ice margin conditions in a narrow and relatively shallow (~60 m deep) fjord valley. Offshore, sedimentation rates over the past 1000 years are an order magnitude much lower (0.032 m/y).

Linking on- and offshore data is challenging. We lack Holocene time control for the offshore fjord infill that can provide sedimentation rates which could be coupled to onshore ice margin and sedimentary infill dynamics during Phase II. The rapidly shifting depocenters are primarily controlled by ice margin location and accommodation space while offshore deposition is expected to be continuous with variable rates.

Acknowledgments

This research was funded by the IPY-NL program of the Netherlands Organisation for Scientific Research (NWO). We would like to thank Alber Hemstede (TUD) and Chris Sprangers for their assistance in the field. We thank Marcel Bakker for contributing data used in this study and for his critical comments. Deltares and T&A radar (Michiel van Oers) are acknowledged for providing the GPR equipment in 2008. Evert Slob and Michael Afanasyev assisted during the GPR data analyses. Antoon Kuijpers (GEUS Denmark) provided the GIMEXMAR'92 core data and radiocarbon samples. OSL dating was facilitated by Jakob Wallinga, Alice Versendaal and Candice Johns of the Netherlands Centre for Luminescence dating (NCL). We like to thank the Kangerlussuaq International Science Support (KISS) facility (Basse Vængtoft) and the Danish IPY Secretariat (Henning Thing) for the local logistics. Information and footage of the field campaigns related to this IPY project can be found at http://pooljaar.nl/rivieren/ (in Dutch).

References

Aarseth, I., 1997. Western Norwegian fjord sediments: age, volume, stratigraphy, and role as temporary depository during glacial cycles. Marine Geology 143, 39–53.

Aebly, F.A., Fritz, S.C., 2009. Palaeohydrology of Kangerlussuaq (Søndre Strømfjord), West Greenland during the last ~8000 years. The Holocene 19, 91–104.

Afanasyev, M., 2009. Imaging Frozen Glacio-fluvial Bedrock Valley Infill Using Ground Penetrating Radar. M.Sc. Thesis, Delft University of Technology, 102 pp.

Alley, R.B., 2000. The younger dryas cold interval as viewed from central Greenland. Quaternary Science Reviews 19, 213–226.

Alley, R.B., Mayewski, P.A., Sowers, T., Stuiver, M., Taylor, K.C., Clark, P.U., 1997. Holocene climatic instability: a prominent, widespread event 8200 yr ago. Geology 25, 483–486.

Anderson, N.J., Leng, M.J., 2004. Increased aridity during the early Holocene in West Greenland inferred from stable isotopes in laminated-lake sediments. Quaternary Science Reviews 23, 841–849.

Axford, Y., Briner, J.P., Miller, G.H., Francis, D.R., 2009. Paleoecological evidence for abrupt cold reversals during peak Holocene warmth on Baffin Island, Arctic Canada. Quaternary Research 71, 142–149. doi:10.1016/j.yqres.2008.09.006.

Bakker, M.A.J., 1996. The Sediments of Søndre Strømfjord and Itivdleq Fjord, West Greenland. Internal Report Geological Survey of the Netherlands. Dept. Marine Geology, Haarlem, 32 pp.

Bierman, P., Corbett, L., Reusser, L., Graly, J., Finkel, R., Rood, D., Neumann, T., March 2010. Quantifying Post-glacial Emergence at Kangerlussuaq, Greenland Using 10-Be Dating of Bedrock Forms Exposed by River Incision. Abstract 40th International Arctic Workshop. INSTAAR, University of Colorado at Boulder, USA.

Bonow, J.M., Lidmar-Bergström, K., Japsen, P., 2006. Palaeosurfaces in central West Greenland as reference for identification of tectonic movements and estimation of erosion. Global and Planetary Change 50, 161–183.

Boulton, G.S., 1990. Sedimentary and sea level changes during glacial cycles and their control on glacimarine facies architecture. In: Dowdeswell, J.A., Scourse, J.D. (Eds.), 1990. Glacimarine Environments: Processes and Sediments. Geological Society, London, Special Publication, vol. 53, pp. 15–52.

Briner, J.P., Stewart, H.A.M., Young, N.E., Philipps, W., Losee, S., 2010. Using proglacial-threshold lakes to constrain fluctuations of the Jakobshavn Isbræ ice margin, western Greenland, during the Holocene. Quaternary Science Reviews 27, 3861–3874.

Cai, J., Powell, R.D., Cowan, E.A., Carlson, P.R., 1997. Lithofacies and seismic-reflection interpretation of temperate glacimarine sedimentation in Tarr Inlet, Glacier Bay, Alaska. Marine Geology 143, 5–37.

Carlson, P.R., 1989. Seismic reflection characteristics of glacial and glacimarine sediment in the Gulf of Alaska and adjacent fjords. Marine Geology 85, 391–416.

Corner, G.D., 2006. A transgressive-regressive model of fjord-valley fill: stratigraphy, facies and depositional controls. In: Dalrymple,, R.W., Leckie,, D.A.,

Tillman,, R.W. (Eds.), 2006. Incised Valleys in Time and Space SEPM Special Publication, vol. 85, pp. 161–178.
Dahl-Jensen, D., Mosegaard, K., Gundestrup, N., Clow, G.D., Johnsen, S.J., Hansen, A.W., Balling, N., 1998. Past temperatures directly from the Greenland Ice Sheet. Science 282, 268–271.
De Winter, I.L., Storms, J.E.A., Overeem, I., in press. Numerical modeling of glacial sediment production and transport during deglaciation. Geomorphology.
Desloges, J.R., Gilbert, R., Nielsen, N., Christiansen, C., Rasch, M., Øhlenschläger, R., 2002. Holocene glacimarine sedimentary environments in fiords of Disko Bugt, West Greenland. Quaternary Science Reviews 21, 947–963.
Dietrich, R., Rülke, A., Scheinert, M., 2005. Present-day vertical crustal deformations in West Greenland from repeated GPS observations. Geophysical Journal International 163, 865–874. doi:10.1111/j.1365-246X.2005.02766.x.
Dijkmans, J.W.A., Törnqvist, T.E., 1991. Modern periglacial eolian deposits and landforms in the Søndre Strømfjord area, West Greenland and their palaeoenvironmental implications. Meddelelser om Grønland. Geoscience 25, 39.
Eilertsen, R., Corner, G.D., Aasheim, O., 2005. Deglaciation chronology and glaciomarine successions in the Malangen-Målselv area, northern Norway. Boreas 34, 233–251.
Eilertsen, R., Corner, G.D., Aasheim, O., Andreassen, K., Kristoffersen, Y., Ystborg, H., 2006. Valley-fill stratigraphy and evolution of the Målselv fjord valley, Northern Norway. In: Dalrymple,, R.W., Leckie,, D.A., Tillman,, R.W. (Eds.), 2006. Incised Valleys in Time and Space SEPM Special Publication, vol. 85, pp. 179–195.
Eisner, W.R., Törnqvist, T.E., Koster, E.A., Bennike, O., van Leeuwen, J.F.N., 1995. Paleoecological studies of a Holocene lacustrine record from the Kangerlussuaq (Søndre Strømfjord) region of West Greenland. Quaternary Research 43, 55–66.
Elverhøi, A., Lønne, Ø., Seland, R., 1983. Glaciomarine sedimentation in a modern fjord environment. Spitsbergen. Polar Research 1, 127–149.
Eyles, N., Mullins, H.T., Hine, A.C., 1991. The seismic stratigraphy of Okanagan Lake, British Columbia; a record of rapid deglaciation in a deep 'fiord-lake' basin. Sedimentary Geology 73, 13–41.
Fleming, K., Lambeck, K., 2004. Constraints on the Greenland Ice Sheet since the Last Glacial Maximum from sea-level observations and glacial-rebound models. Quaternary Science Reviews 23, 1053–1077.
Foreman, S.L., Marin, L., van der Veen, C., Tremer, C., Scatho, B., 2007. Little Ice Age and neoglacial landforms at the Inland Ice margin, Isunguata Sermia, Kangerlussuaq, west Greenland. Boreas 36, 1–11. doi:10.1080/00173130601173301.
Funder, S., Hansen, L., 1996. The Greenland ice sheet – a model for its culmination and decay during and after the last glacial maximum. Bulletin of the Geological Society of Denmark 42, 137–152.
Gilbert, R., 1985. Quaternary glaciomarine sedimentation interpreted from seismic surveys of fiords on Baffin Island, N.W.T. Arctic 38, 271–280.
Hallet, B., Hunter, L., Bogen, J., 1996. Rates of erosion and sediment evacuation by glaciers: a review of field data and their implications. Global and Planetary Change 12, 213–235.
Hansen, L., Beylich, A., Burki, V., Eilertsen, R.S., Fredin, O., Larsen, E., Lyså, A., Nesje, A., Stalsberg, K., Tønnesen, J.F., 2009. Stratigraphic architecture and infill history of a deglaciated bedrock valley based on georadar, seismic profiling and drilling. Sedimentology. doi:10.1111/j.1365-3091.2009.01056.x.
Helle, S.K., 2004. Sequence stratigraphy in a marine moraine at the head of Hardangerfjorden, western Norway: evidence for a high-frequency relative sea-level cycle. Sedimentary Geology 164, 251–281.
Jol, H.M., Bristow, C.S., 2003. GPR in sediments: advice on data collection, basic processing and interpretation, a good practice guide. In: Bristow, C.S., Jol, H.M. (Eds.), 2003. Ground Penetrating Radar in Sediments, Geolological Society, London, Special Publication, vol. 211, pp. 9–27.
Kaufman, D.S., Ager, T.A., Anderson, N.J., Anderson, P.M., Andrews, J.T., Bartlein, P.J., Brubaker, L.B., Coats, L.L., Cwynar, L.C., Duvall, M.L., Dyke, A.S., Edwards, M.E., Eisner, W.R., Gajewski, K., Geirsdóttir, A., Hu, F.S., Jennings, A.E., Kaplan, M.R., Kerwin, M.W., Lozhkin, A.V., MacDonald, G.M., Miller, G.H., Mock, C.J., Oswald, W.W., Otto-Bliesner, B.L., Porinchu, D.F., Rühland, K., Smol, J.P., Steig, E.J., Wolfe, B.B., 2004. Holocene thermal maximum in the western Arctic (0–180° W). Quaternary Science Reviews 23, 529–560.
Kelly, M., 1985. A review of the Quaternary geology of western Greenland. In: Andrews, J.T. (Ed.), Quaternary Environments, Eastern Canadian Arctic, Baffin Bay and Western Greenland, pp. 461–501.
Kelly, M., 1988. The Status of Neoglacial in Western Greenland. In: Rapport Grønlands Geologiske Undersøgelse, vol. 96, 24 pp.
Kneller, B., 2003. The influence of flow parameters on turbidite slope channel architecture. Marine and Petroleum Geology 20, 901–910.
Knight, P.G., Waller, R.I., Patterson, C.J., Jones, A.P., Robinson, Z.P., 2000. Glacier advance, ice-marginal lakes and routing of meltwater and sediment: Russell Glacier, Greenland. Journal of Glaciology 46, 423–426.
Larsen, B., 1977. Investigations of the sediment thickness in Søndre Strømfjord, West Greendland. Grønlands Geologiske Undersøgelse 85, 47–48.
Long, A.J., Roberts, D.H., Dawson, S., 2006. Early Holocene history of the west Greenland Ice Sheet and the GH-8.2 event. Quaternary Science Reviews 25, 904–922.
Long, A.J., Woodroffe, S.A., Dawson, S., Roberts, D.H., Bryant, C.L., 2009. Late Holocene relative sea level rise and the Neoglacial history of the Greenland ice sheet. Journal of Quaternary Science 24, 345–359.
Long, A.J., Woodroffe, S.A., Milne, G.A., Bryant, C.L., Wake, L.M., 2010. Relative sea level change in west Greenland during the last millennium. Quaternary Science Reviews 29, 367–383.
Lyså, A., Vorren, T.O., 1997. Seismic facies and architecture of ice-contact submarine fans in high-relief fjords, Troms, Northern Norway. Boreas 26, 309–328.
Lyså, A., Sejrup, H.P., Aarseth, I., 2004. The late glacial-Holocene seismic stratigraphy and sedimentary environment in Ranafjorden, northern Norway. Marine Geology 211, 45–78.
Lønne, I., 1995. Sedimentary facies and depositional architecture of ice-contact glaciomarine systems. Sedimentary Geology 98, 13–43.
McGowan, S., Ryves, D.B., Anderson, N.J., 2003. Holocene records of effective precipitation in West Greenland. The Holocene 13, 239–249.
McGrath, D., Steffen, K., Overeem, I., Mernild, S.H., Hasholt, B., Van Den Broeke, M., 2010. Sediment plumes as a proxy for local ice-sheet runoff in Kangerlussuaq Fjord, West Greenland. Journal of Glaciology 56, 813–821.
McNeely, R., Dyke, A.S., Southon, J.R., 2006. Canadian marine reservoir ages, preliminary data assessment, Open File 5049. Geological Survey Canada.
Mernild, S.H., Hasholt, B., 2009. Observed runoff, jökulhlaups, and suspended sediment load from the Greenland Ice Sheet at Kangerlussuaq, West Greenland, for 2007 and 2008. Journal of Glaciology 55, 855–858.
Muto, T., Steel, R.J., 1992. Retreat of the front in a prograding delta. Geology 20, 967–970.
Ó Cofaigh, C., Dowdeswell, J.A., Grobe, H., 2001. Holocene glacimarine sedimentation, inner Scoresby Sund, East Greenland: the influence of fast-flowing ice-sheet outlet glaciers. Marine Geology 175, 103–129.
Oele, E., 1992. GIMEXMAR '92 Cruise Report. Geological Survey of the Netherlands, Marine Geology Division, Haarlem.
Overeem, I., Syvitski, J.P.M., 2010. Experimental exploration of the stratigraphy of fjords fed by glaciofluvial systems. In: Howe, J.A., Austin, W.E.N., Forwick, M., Paetzel, M. (Eds.), 2010. Fjord Systems and Archives. Geological Society, London, Special Publications, vol. 344, pp. 127–144.
Overeem, I. Briner, J.P., Kettner, A.J., Syvitski, J.P.M., in preparation. Valley filling during deglaciation: a case-study of Clyde fjordhead, Baffin Island, Arctic Canada.
Plassen, L., Vorren, T.O., 2003. Sedimentary processes and the environment during deglaciation of a fjord basin in Ullsfjorden, Northern Norway. Norwegian Journal of Geology 83, 23–36.
Powell, R.D., 1990. Glacimarine processes at grounding-line fans and their growth to ice-contact deltas. In: Dowdeswell, J.A., Scourse, J.D. (Eds.), 1990. Glacimarine Environments: Processes and Sediments. Geol. Soc. Spec. Publ, vol. 53, pp. 53–73.
Powell, R.D., Molnia, B.F., 1989. Glacimarine sedimentary processes, facies and morphology of the south-southeast Alaska shelf and fjords. Marine Geology 85, 359–390.
Prior, D.B., Bornhold, B.D., Johns, M.W., 1986. Active sand transport along a fjord-bottom channel, Bute inlet, British Columbia. Geology 14, 518–584.
Russell, A.J., 1989. A comparison of two recent jokulhlaups from an-ice-dammed lake, Sondre Stromfjord, West Greenland. Journal of Glaciology 35, 157–162.
Russell, A.J., 2007. Controls on the sedimentology of an ice-contact jökulhlaup-dominated delta, Kangerlussuaq, West Greenland. Sedimentary Geology 193, 131–148.
Russell, A.J., 2009. Jökulhlaup (ice-dammed lake outburst flood) impact within a valley-confined sandur subject to backwater conditions, Kangerlussuaq, West Greenland. Sedimentary Geology 215, 33–49.
Russell, A.J., van Tatenhove, F.G.M., van der Wal, R.S.W., 1995. Effects of ice-front collapse and flood generation on a proglacial River channel near Kangerlussuaq (Sondre Stromfjord), West Greenland. Hydrological Processes 9, 213–227.
Sandmeier, K.J., 2007. REFLEXW – Program for Processing and Interpretation of Reflection and Transmission Data, Manual, Version 4.5.
Scholz, H., Grottenthaler, W., 1989. Contributions to the earlier Holocene deglaciation history in central West Greenland. Polar Geography 13, 22–41.
Simpson, M.J.R., Milne, G.A., Huybrechts, P., Long, A.J., 2009. Calibrating a glaciological model of the Greenland Ice Sheet from the Last Glacial Maximum to present-day using field observations of relative sea level and ice extent. Quaternary Science Reviews 28, 1631–1657.
Stuiver, M., Reimer, P.J., Reimer, R.W., 2005. CALIB 6.0. Program Documentation. http://calib.qub.ac.uk/calib/.
Sugden, D., 1972. Deglaciation and isostacy in the Sukkertoppen Ice Cap area, west Greenland. Arctic and Alpine Research 4, 97–117.
Syvitski, J.M.P., Lee, H.J., 1997. Postglacial sequence stratigraphy of Lake Melville, Labrador. Marine Geology 143, 55–79.
Tarasov, L., Peltier, W.R., 2002. Greenland glacial history and local geodynamic consequences. Geophysical Journal International 150, 198–229.
Tarasov, L., Peltier, W.R., 2003. Greenland glacial history, borehole constraints, and Eemian extent. Journal of Geophysical Research 108 (B3), 2143. doi:10.1029/2001JB001731.
Ten Brink, N.W., 1974. Glacio-isostacy: new data from west Greenland and geophysical implications. Geological Society of America Bulletin 85, 219–228.
Ten Brink, N.W., 1975. Holocene history of the Greenland ice sheet based on radiocarbon-dated moraines in west Greenland. Grønlands Geologiske Undersøgelse Bulletin 113, 44.
Ten Brink, N.W., Weidick, A., 1974. Greenland ice sheet history since the last deglaciation. Quaternary Research 4, 429–440.
Van der Meer, J.J.M., van Tatenhove, F.G.M., Laban, C., 1993. Glaciation and Isostasy in the Søndre Strømfjord – Itivdlq System. In: Grønlands Geologiske Undersøgelse Open File Series 93/5, 84–86 pp.
Van der Meer, J.J.M., van der Borg, K., Laban, C., van Tatenhove, F.G.M., 1994. Dating Deglaciation and its Aftermath in Søndre Strømfjord/Sandflugtdalen. In: Grønlands Geologiske Undersøgelse Open File Series 94/13, 77–80 pp.
Van Heteren, S., FitzGerald, D.M., McKinlay, P.A., Buynevich, I.V., 1998. Radar facies of paraglacial barrier systems: coastal New England, USA. Sedimentology 45, 181–200.

Please cite this article in press as: Storms, J.E.A., et al., The Holocene sedimentary history of the Kangerlussuaq Fjord-valley fill, West Greenland, Quaternary Science Reviews (2012), doi:10.1016/j.quascirev.2011.12.014

Van Tatenhove, F.G.M., 1995. The Dynamics of Holocene Deglaciation in West Greenland with Emphasis on Recent Ice-marginal Processes. PhD Thesis, University of Amsterdam. ISBN 90-6787-039-0. 202 p.

Van Tatenhove, F.G.M., van der Meer, J.J.M., Koster, E.A., 1996. Implications for deglaciation chronology from new AMS age determinations in central west Greenland. Quaternary Research 45, 245–253.

Vinther, B.M., Buchardt, S.L., Clausen, H.B., Dahl-Jensen, D., Johnsen, S.J., fisher, D.A., Koerner, R.M., Raynaud, D., Lipenkov, V., Andersen, K.K., Blunier, T., Rasmussen, S.O., Steffensen, J.P., Svensson, A.M., 2009. Holocene thinning of the Greenland ice sheet. Nature 461, 385–388. doi:10.1038/nature08355.

Weidick, A., 1985. Review of glacier changes in West Greenland. Zeitschrift für Gletscherkunde und Glazialgeologie 21, 301–309.

Weidick, A., 1993. Neoglacial Change of Ice Cover and the Related Response of the Earth's Crust in West Greenland. In: Grønlands Geologiske Undersøgelse Rapport, vol. 159, 121–126 pp.

Willemse, N.W., Törnqvist, T.E., 1999. Holocene century-scale temperature variability from West Greenland lake records. Geology 27, 580–584.

Willemse, N.W., Koster, E.A., Hoogakker, B., van Tatenhove, F.G.M., 2003. A continuous record of Holocene eolian activity in West Greenland. Quaternary Research 59, 322–334.

Please cite this article in press as: Storms, J.E.A., et al., The Holocene sedimentary history of the Kangerlussuaq Fjord-valley fill, West Greenland, Quaternary Science Reviews (2012), doi:10.1016/j.quascirev.2011.12.014